Downloaded from rsta.royalsocietypublishing.org

PHILOSOPHICAL TRANSACTIONS OF THE ROYAL SOCIETY A MATHEMATICAL, PHYSICAL & ENGINEERING SCIENCES

A New Determination of the Gas Constant by an Acoustical Method

T. J. Quinn, A. R. Colclough and T. R. D. Chandler

Phil. Trans. R. Soc. Lond. A 1976 **283**, 367-420
doi: 10.1098/rsta.1976.0090

Email alerting service

Receive free email alerts when new articles cite this article - sign up in the box at the top right-hand corner of the article or click **here**

To subscribe to *Phil. Trans. R. Soc. Lond. A* go to: **http://rsta.royalsocietypublishing.org/subscriptions**

This journal is © 1976 The Royal Society

Downloaded from rsta.royalsocietypublishing.org

A NEW DETERMINATION OF THE GAS CONSTANT BY AN ACOUSTICAL METHOD

By T. J. Quinn, A. R. Colclough and T. R. D. Chandler
Division of Quantum Metrology, National Physical Laboratory, Teddington, Middlesex

(*Communicated by J. Dyson, F.R.S. – Received* 16 *June* 1975)

[Plate 1]

CONTENTS

A new determination of the gas constant has been made using a method in which the velocity of sound in argon was measured by means of an acoustic inteferometer operated at a temperature close to 273.16 K. Ninety-eight independent velocity measurements were made over a pressure range from 30 to 200 kPa to enable the velocity at zero pressure to be deduced by extrapolation. By using this experimental value, a new value for the gas constant of $8315.73 \pm 0.17\,\mathrm{J\,K^{-1}\,kmol^{-1}}$ was deduced. This is higher than the old value for R, obtained from measurements of the density of oxygen, by 159 p.p.m. (parts/10^6).

The Royal Society is collaborating with JSTOR to digitize, preserve, and extend access to *Philosophical Transactions of the Royal Society of London. Series A, Mathematical and Physical Sciences.* www.jstor.org

Downloaded from rsta.royalsocietypublishing.org

1. Introduction

The gas constant, R, enters into the set of physical constants as the link between thermal and mechanical quantities through the Boltzmann constant, k (equal to R/N_A, where N_A is the Avogadro number). The rôle of the gas constant can most easily be seen in the equation of state of an ideal gas, namely

$$pv = nRT = nN_A kT, \tag{1}$$

where p and v are the pressure and volume respectively, n the number of moles of gas and T the thermodynamic temperature. The numerical values of p and v are a consequence of the choice of the base units of mass, length and time and so the numerical value of R depends upon the unit of temperature. For historical and practical reasons, the numerical value of the temperature of a convenient reference state is defined and the gas constant is measured experimentally in terms of p, v, n and T. The reference state chosen is the triple point of water, which now has a defined thermodynamic temperature of 273.16 K. In principle any system having an exactly specifiable number of internal degrees of freedom at a known thermodynamic temperature could be used to determine the value of the gas constant or Boltzmann's constant. It should be noted that although a value for N_A is required to separate R from k, the accuracy with which N_A is known, is substantially better than that associated with the experimental measurements of R or k. Recent values based upon X-ray diffraction work have associated uncertainties at the 1 p.p.m. level (Cohen & Taylor 1973; Deslattes 1976). An experimental determination of k can therefore be considered as giving an equal amount of information about R and vice versa.

The temperature at which a determination of R or k can be undertaken is limited in practice because our knowledge of thermodynamic temperature away from the triple point is too inaccurate. For example, recent measurements of the thermodynamic temperature of the steam point by Guildner & Edsinger (1973) have given a value of 99.97 °C, which is 0.03 °C lower than the conventional value.† If their results are substantiated then the change will be equivalent to a proportional error of about 80 p.p.m. in our knowledge of thermodynamic temperature at this point. Since this work shows the error over the range 0 to about 140 °C to be almost linearly proportional to temperature, we can consider the thermodynamic temperature near 25 °C to be uncertain, for the time being, by 20 p.p.m.

Concerning the physical rôle of the constants R and k, it should be pointed out that a knowledge of their value is not, in principle, required for the determination of thermodynamic temperature provided that the method chosen is one based simply upon the ratio of the measured thermometric quantity at temperatures T and T_0. For example, the ratio of the total thermal radiation energy (E_T) emitted by a black body at temperature T to that at T_0, the reference temperature, is given by

$$\frac{E_T}{E_{T_0}} = \frac{T^4}{T_0^4}. \tag{2}$$

A measurement of T by a single absolute determination of E_T would, on the other hand, require a knowledge of k for, in the conventional notation,

$$E_T = \frac{2\pi^5}{15}\frac{k^4}{c^2h^3}T^4. \tag{3}$$

† The steam point ceased to be a defined temperature in 1954 (Hall & Barber 1967) when the unit of thermodynamic temperature was redefined as 1/273.16 of the interval between absolute zero and the triple point of water. Before then absolute zero was, oddly enough, a temperature which was experimentally determined in terms of the ice point–steam point interval.

Downloaded from rsta.royalsocietypublishing.org

But since
$$k^4 = \frac{15c^2h^3}{2\pi^5 T_0^4} E_{T_0}, \tag{4}$$
we are implicitly comparing E_T with E_{T_0} using k as the intermediary constant. Similar arguments may be produced for a gas thermometer, acoustic thermometer, Johnson noise thermometer or any other thermometer. We can therefore see that in any measurement which links a thermal quantity *directly* with a mechanical quantity (as in equation (3)) a knowledge of k is required. But for a measurement which involves only a ratio of thermal quantities (as in equation (2)) no such knowledge is needed. Herein lies the practical usefulness of the constants k or R – they obviate the need for a measurement at T_0 in a wide range of experimental situations. A similar chain of reasoning holds if we consider systems in which chemical changes take place. In principle k or R could be determined from absolute measurements of rates of chemical reactions involving measurements of quantities of substance. For the time being, however, methods of this sort pose even greater difficulties than do the physical methods used so far for the measurement of k and R.

The presently accepted value for R stems from measurements of the density of oxygen carried out by three groups of workers between 1924 and 1949. These density measurements were made in order to arrive at a value for the molar volume, V. In the limit of low pressures, Vp/P_0 approaches the normal molar volume of an ideal gas V_0 which is related to R by the equation of state
$$P_0 V_0 = RT_0, \tag{5}$$
where P_0 is one standard atmosphere and T_0 is 273.15 K.† Since no real gas is a sufficiently good approximation to an ideal gas at P_0 and T_0 the experimental method has to be one which makes use of the approach to ideal behaviour which real gases exhibit in the limit of low pressures.

For an ideal gas the molar volume and molecular mass M are related by
$$M = L_0 V_0, \tag{6}$$
where L_0 is the density of the gas at P_0 and T_0. For a given mass m of a real gas the density ρ_p at any pressure p is given by
$$\rho_p = \frac{m}{v}. \tag{7}$$
We may therefore define a quantity L_p by
$$L_p = \frac{P_0}{p}\rho_p = \frac{P_0}{p}\frac{m}{v}, \tag{8}$$
so that when $p = P_0$ we have
$$L_1 = \frac{m}{v} \tag{9}$$
(see figure 1).

Since the departures from ideal behaviour tend to zero as p tends to zero it is apparent from equation (8) and figure 1 that in the limit of low pressures
$$L_p \to L_0$$
for all gases. Experimental measurements of ρ_p at successively lower pressures can therefore be used to arrive at a value for L_0 and so to obtain V_0 for a given value of M.

At the time the experimental work was done the most suitable experimental gas was oxygen whose molecular mass was then defined to be 16. Since the physical scale of atomic masses was adopted in 1961 it has become possible to consider using other gases. The main requirement is that the isotopic composition of the proposed gas be well established and invariant within the

† Since V_0 is conventionally defined at s.t.p. we now take $T_0 = 273.15$ K (the ice point) rather than 273.16 K.

PHILOSOPHICAL TRANSACTIONS OF THE ROYAL SOCIETY A MATHEMATICAL, PHYSICAL & ENGINEERING SCIENCES
PHILOSOPHICAL TRANSACTIONS OF THE ROYAL SOCIETY A MATHEMATICAL, PHYSICAL & ENGINEERING SCIENCES

Downloaded from rsta.royalsocietypublishing.org

limits required for the molecular mass calculation. This is a severe limitation since most of the heavier gases have too many isotopes for present mass spectrometry techniques to be used to determine their relative isotopic composition with sufficient accuracy.

The most recent experimental work on the determination of the limiting density of oxygen is that of Batuecas and his collaborators carried out during the period extending from 1941 to 1949. The results were originally published in 1950 and 1952 (Batuecas & Malde 1950; Batuecas 1952) but have been revised on a number of occasions to bring them up to date and correct small errors.

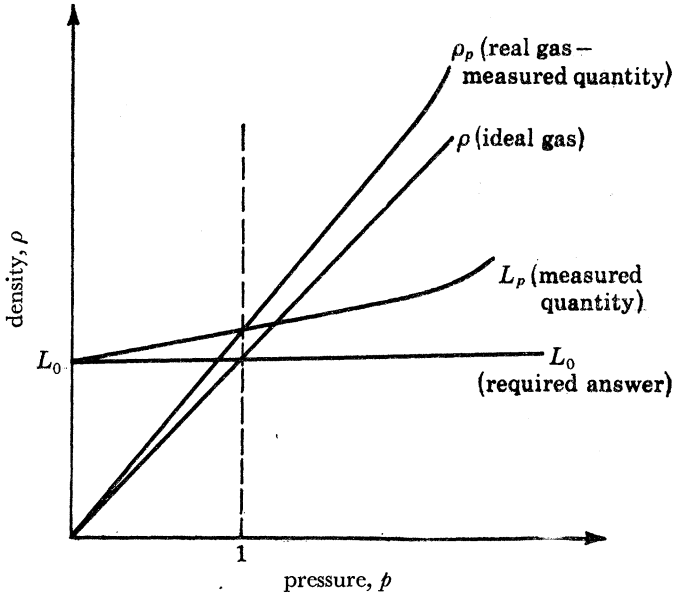

FIGURE 1. The relation between ρ, L_0 and ρ_p, L_p.

The most recent recalculation appeared in the Proceedings of the 4th Conference on Atomic Masses (AMCO-4) in 1971 (Batuecas 1972). In this review Batuecas also presented the results of his recalculation of the work of Baxter & Starkweather (1924, 1926) and of Moles (1938). He concluded that as a result of the very good agreement between all the recalculated results, the most probable value of the normal molecular volume of an ideal gas is

$$22.4132 \pm 0.0007\,\mathrm{l\,atm\,mol^{-1}} \quad (1\,\mathrm{atm} \approx 10^5\,\mathrm{Pa}).$$

The error quoted, equivalent to 31 p.p.m., represents only the statistical standard error of the experimental results, no estimate of systematic errors being given.

It is the opinion of the present authors, however, that an examination of the original experimental results of both Batuecas and collaborators and Baxter & Starkweather leads to the conclusion that the close agreement between their results is probably fortuitous and that the uncertainty quoted above should be somewhat larger. Unfortunately the original results of Moles were published in the proceedings of a conference (1938), a copy of which we have been unable to obtain and so a detailed comparison with his estimate of error has been impossible.

Taking first the results of Baxter & Starkweather we find that there are a number of unusual features present which make a proper assessment of their results very difficult. In figure 2 we show their original experimental results for L_p $(= \rho_p P_0/p)$ plotted against pressure. Each point was obtained by taking their values for L_p and p from the tables in their paper. The authors stated that

Downloaded from rsta.royalsocietypublishing.org

the results for L_p presented at a pressure of 0.75 atm were obtained either at 0.82 or 0.68 atm, and were subsequently corrected to a pressure of 0.75 atm by using the accepted expansion coefficient of oxygen. (A pressure of 0.75 atm was outside the range of both their high pressure and low pressure barometers.) No indication was given regarding which of the results originated at the higher pressure and which at the lower. It is clear from figure 2 that the distribution of the results

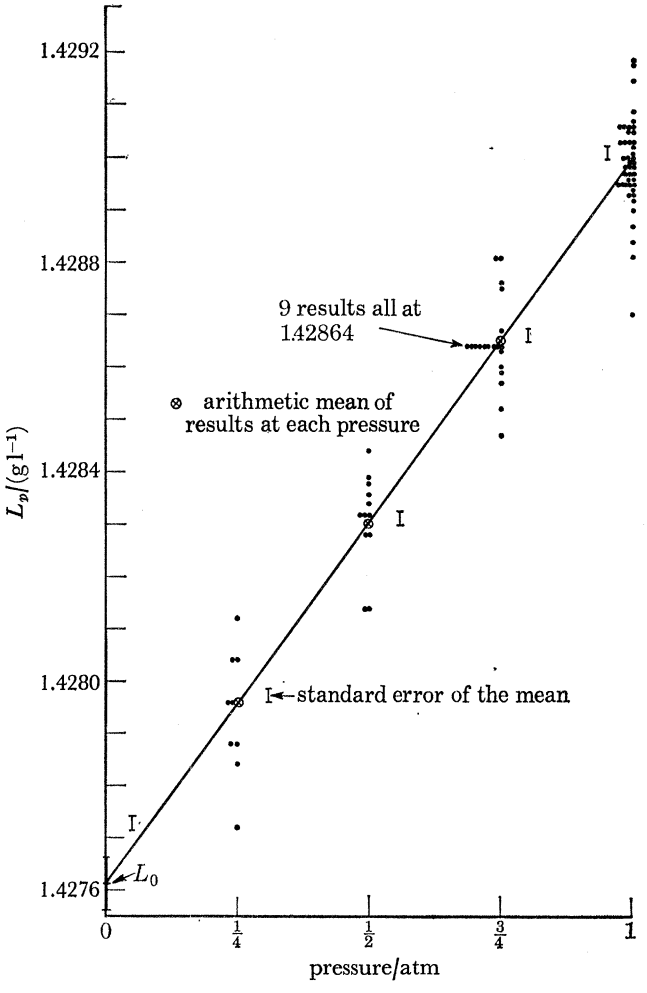

FIGURE 2. The original experimental results of Baxter & Starkweather (1924, 1926), L_p against pressure.

at 0.75 atm is anything but random. Of the twenty experimental results reported, which range from 1.42843 to 1.42881 g l^{-1}, nine have the identical numerical value of 1.42864. Despite this the arithmetic mean of all the measurements at this pressure differs by only 1 p.p.m. from that predicted by a straight line made to pass exactly through the arithmetic means of the results at 0.25 and 1.0 atm. The arithmetic mean of the results at 0.5 atm is 5 p.p.m. above the value predicted by the same straight line. The standard errors of the mean associated with the sets of results at 0.75 and 0.5 atm are both about 20 p.p.m. The results at 0.75 atm seem to be made up of samples of two populations having a widely differing variance and so an overall standard error of the mean is of little significance. In the absence of any explanation of the unusual character of these results or any discussion by the authors of possible sources of systematic error we do not

Downloaded from rsta.royalsocietypublishing.org

think that any weight can be attached to the close agreement between their result and that of Batuecas and co-workers.

In figure 3 we show the original results of Batuecas & Malde (1950) taken from tables II, III and IV of their paper. Existing knowledge of the departure from ideal behaviour of oxygen in this pressure range predicts that L_p should indeed be linearly proportional to pressure within the required limits of accuracy. The estimates of error quoted by Batuecas all appear to be based upon

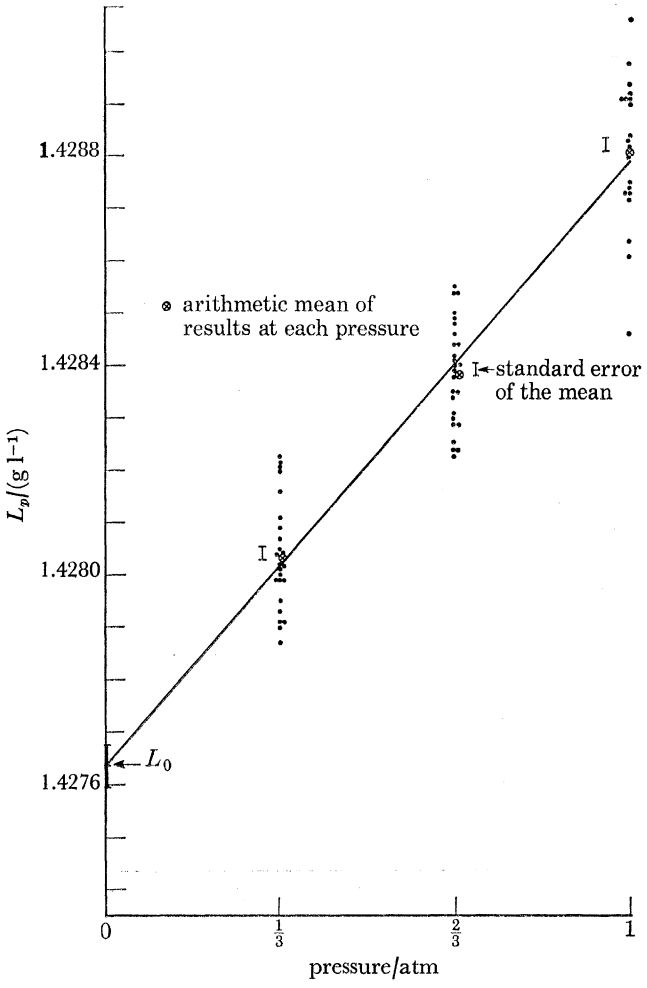

FIGURE 3. The original experimental results of Batuecas & Malde (1950, 1952), L_p against pressure.

the random error of the experimental results. No discussion is given of possible sources of systematic error so it is again difficult to come to any conclusions regarding the source of the difference between his results and ours. There is little doubt, however, that the difference of 159 p.p.m. is significant since it is approximately five times Batuecas' statistical standard error and nearly eight times ours.

The difficulties inherent in precise measurements of the extensive parameters of a gas have recently been highlighted by work at the National Bureau of Standards (N.B.S.) on constant volume gas thermometry. Guildner & Edsinger (1973) have demonstrated that sorption can lead

Downloaded from rsta.royalsocietypublishing.org

to systematic errors in gas thermometry whose presence is by no means obvious. Their work has been carried out in the temperature range from 0 up to 400 °C and is therefore of direct relevance to all the previous oxygen density work related to the gas constant. In the light of their experience of the difficulties of adequately pumping a system in which a relatively large container is connected to pressure measuring devices by means of a tube of small diameter, it is clear that an alternative method for the determination of the gas constant is desirable.

It was because of the very considerable experimental problems associated with measuring the extensive parameters of the gas sample, that it was decided to approach the problem acoustically. The velocity of sound, c_0, in an unbounded ideal gas is related to the gas constant by:

$$c_0^2 = \frac{\gamma RT}{M}, \tag{10}$$

where γ is the ratio of the principal specific heats. Both c_0 and T are intensive thermodynamic quantities and quite independent of the experimentally elusive bulk quantities. In principle, it is not even necessary to measure T since the velocity of sound may be determined at the triple point of water where, by definition, $T = 273.16$ K. It is easy to evaluate γ theoretically for a simple gas and M may be obtained with sufficient accuracy provided that a suitable gas is chosen having a known isotopic composition.

In practice allowance must be made for the non-ideality of the gas. Measurement of the velocity of sound at pressures low enough to make the effect of the virial coefficients negligible is not possible with sufficient sensitivity, and so acoustic isotherms of c^2 against pressure are plotted at comparatively high pressures and extrapolated to zero pressure to obtain c_0^2. c^2 can be shown to take the following form

$$c^2 = A_0(T) + A_1(T)\,p + A_2(T)\,p^2 + \ldots, \tag{11}$$

where $A_0(T) = \gamma RT/M$, $A_1(T), A_2(T), \ldots$ are referred to as the first, second, third, etc. acoustic virial coefficients by analogy with those in the virial expansion of the product pv; the familiar form of the equation of state for a real gas. Explicit relations are given and discussed in § 6 of this paper in which the acoustic virial coefficients are written down in terms of the virial coefficients proper, and their derivatives with respect to T (Colclough 1973). These might, in principle, be used to correct velocities measured at finite pressures to the ideal gas values. However, they involve the first and second derivatives with respect to temperature of both the second and third virial coefficients and, as we shall see, these are not sufficiently well known for our purpose. Moreover, it is always desirable that a new determination of a fundamental constant be carried out with a minimum of reliance being placed upon external experimental data.

2. The acoustical method

2.1. *The choice of method*

The choice of a low frequency variable path acoustic interferometer for the measurement of sound velocity was based upon the experience we have had in using such an instrument for another purpose. For some years work has been underway both at the N.P.L. and the N.B.S. on the acoustic determination of thermodynamic temperature in the range 2–20 K. Following an extensive study, both theoretical and experimental, of the systematic errors of acoustic thermometry we designed the instrument described here for the measurement of the gas constant. The

Downloaded from rsta.royalsocietypublishing.org

arguments, given in detail in the earlier paper (Colclough 1973), for the choice of a low frequency acoustic interferometer may be summarized briefly as follows:

(*a*) A standing wave method has many advantages over a time of flight method both from the point of view of space and of control over many experimental parameters.

(*b*) A variable path interferometer operated at a fixed frequency is preferable to a fixed path interferometer with a variable frequency. The disadvantage of the latter method lies in the requirement for a knowledge of the absolute acoustic length of the cavity whereas in the former it is only changes in length which need be measured. As will be seen later the boundary layer corrections at the end faces of a variable path interferometer are constant and do not enter into the calculation of the wavelength. Moreover, in the case of the fixed frequency instrument the mechanical impedance of the transducer remains constant from one order of resonance to the next.

Colclough (1972, 1973) has shown that flat, but tilted end faces result in no phase change on reflexion for an instrument operated below the first cut-off frequency. Phase changes occur only through lack of flatness at the end faces. However, in a variable path device, it is the separation of resonances which are measured and set equal to $\frac{1}{2}\lambda$. Thus phase changes occurring on reflexion are of no consequence in any case. Tilted end faces do, however, result in an amplitude loss on reflexion given by $2\pi^2 b^2 \chi^2/\lambda^2$ where χ is the angle of tilt in radians and b the radius of the cavity. A value of $\chi \approx 10^{-3}$ rad should be achieved with no difficulty whatsoever so that if $\lambda/b \approx 3.3$ the loss is approximately 2×10^{-6} per reflexion, which is small compared to the boundary layer loss.

(*c*) We chose a low frequency interferometer because the high frequency method, despite certain advantages stemming from the possibility of using a resonating quartz crystal transducer, suffers from the overriding disadvantage of having systematic errors which are not reliably assessable. At frequencies in excess of many of the characteristic cut-off frequencies of the cavity there is no guarantee that a true plane wave phase velocity is being measured. It is much more likely to be a group velocity constituted of the phase velocities of many of the higher modes of propagation which may be excited. There appear to be no checks which may be made in practice either on the transducer or on the form of the resonance curve to ensure that this is not the case. Moreover, the alignment of cavity end faces in the ultrasonic instrument is not a simple matter. Usually this is done optically to ensure that the distance 'out of true' of any point on a tilted end face is small compared to the acoustic wavelength (10^{-2} cm, say). However, the theory of the device predicts that the halfwidths of the resonance peaks may be of the order of wavelengths of light. Detailed analysis shows that alignment requirements are more stringent than usually supposed (Colclough 1976). The low frequency interferometer (i.e. one operated below the lowest cut-off frequency) does not suffer from these problems. Only the plane wave may propagate so that no ambiguity arises in the composition of the wave field.

2.2. *The acoustic boundary layer*

The advantages of the low frequency instrument are, however, paid for by incurring the problem associated with the acoustic boundary layer. Due to the viscosity of the gas in the cavity and the high thermal diffusivity of the cavity walls, which tend to make propagation isothermal rather than adiabatic in their neighbourhood, the measured velocity of sound is less than that in the unbounded fluid. In addition, acoustic absorption is increased – to such an extent that the boundary layer loss predominates over the classical absorption arising from heat flow and viscosity in the body of the gas rather than at the walls, the latter being almost negligible in comparison. A boundary layer loss and phase change also occur on reflexion at the cavity end

Downloaded from rsta.royalsocietypublishing.org

faces. Expressions for the boundary layer velocity change and absorption coefficients were originally derived by Kirchhoff (1868) and Helmholtz (1863). We prefer to quote them in the following form:

$$c = c_0(1-\alpha_{\mathrm{K.H.}}/k_0) \tag{12}$$

giving

$$\Delta c \equiv c_0 - c = \frac{\alpha_{\mathrm{K.H.}} c_0^2}{\omega} \doteq \frac{\alpha_{\mathrm{K.H.}} c^2}{\omega}\left(1+\frac{2\alpha_{\mathrm{K.H.}} c}{\omega}\right) \tag{13}$$

for the correction to the measured velocity, c, where the Kirchhoff–Helmholtz boundary layer absorption coefficient is calculated from

$$\alpha_{\mathrm{K.H.}} = \frac{1}{bc_0}\left\{\nu^{\frac{1}{2}} + (\gamma-1)\left(\frac{K}{\rho c_p}\right)^{\frac{1}{2}}\right\}\left\{\frac{\omega}{2}\right\}^{\frac{1}{2}} \tag{14}$$

and where ν is the kinematic viscosity, b the cavity radius, K the thermal conductivity, c_p the specific heat at constant pressure, k_0 the wavenumber for the unbounded fluid and ω the angular frequency. In our argon filled interferometer for which $b = 1.5\,\mathrm{cm}$ we therefore expect $\Delta c/c$ at 273 K to be 1.1×10^{-3} at 200 kPa and 2.7×10^{-3} at 30 kPa: the upper and lower limits of our acoustic isotherm (table 3).

The orthodox boundary layer theory does, however, make some small approximations which have been investigated in detail by Shields, Lee & Wiley (1965). They carried out a direct numerical solution of the fundamental fluid mechanical equations thus avoiding the approximations implicit in the usual formulation of the Kirchhoff–Helmholtz results. These results, they argue, predict too large a velocity decrease for sound propagated in tubes and too small an absorption coefficient. For an instrument such as ours the fractional error in a calculated correction $\Delta c/c$ would be 1.0 $\Delta c/c$ and for a calculated value of $\alpha_{\mathrm{K.H.}}$ would be 2.4 $\Delta c/c$, i.e. errors in c and $\alpha_{\mathrm{K.H.}}$ of order $(\Delta c/c)^2$. Owing to our using a measured boundary layer absorption coefficient in conjunction with equation (12) to make the velocity correction (see below), we have to decrease the Kirchhoff–Helmholtz velocity correction by a fraction 3.4 $\Delta c/c$ rather than 1.0 $\Delta c/c$. We also follow Shields *et al.* in making a small correction for molecular slip (see § 5).

Thiesen (1907) added a further term to the velocity correction to allow for the effect of the boundary layer at the end faces:

$$-\frac{c(\gamma-1)}{l}\left(\frac{K}{\rho c_p}\right)^{\frac{1}{2}}\left(\frac{\omega}{2}\right)^{-\frac{1}{2}}, \tag{15}$$

where l is the length of the acoustic cavity. The latter correction has occasionally been misunderstood. It should be made only where the measured geometrical length of the cavity is used in the calculation of the velocity of sound as it would be, for example, in the case of a fixed path/variable frequency interferometer. If the separations of the positions of resonance are measured in a variable path device, on the other hand, the correction need not be made. To see this more clearly we express the boundary layer reflexion coefficient, $\sigma\,\mathrm{e}^{\pm\mathrm{i}\delta}$ in the following form:

$$\sigma = 1-\frac{(\gamma-1)}{c}\left(\frac{K}{\rho c_p}\right)^{\frac{1}{2}}(2\omega)^{\frac{1}{2}}, \tag{16}$$

$$\delta = -\frac{(\gamma-1)}{c}\left(\frac{K}{\rho c_p}\right)^{\frac{1}{2}}(2\omega)^{\frac{1}{2}}, \tag{17}$$

Downloaded from rsta.royalsocietypublishing.org

where σ represents the loss and δ a phase change (the sign being chosen according to whether reflexion is from the left or the right). Thiesen's term arises from δ as may easily be seen, and, being a phase change, may be represented by a slight imaginary displacement of the end face from its true position – hence the need for a correction to the measured cavity length. This theory of boundary layer reflexion has been treated by Herzfeld (1931).

Unfortunately, and in our view, needlessly, the simple theory of the acoustic boundary layer due to Kirchhoff and Helmholtz has been widely regarded with suspicion. The doubt seems to have arisen with some work performed as long ago as 1869 and 1870 by Schneebeli and Seebeck (1869, 1870) with very primitive, powder filled, mechanically excited, glass interferometers. Even assuming the roughness of the walls to have been small compared with the boundary layer thickness, a dusting of lycopodium powder could have been relied upon to make them acoustically rough. The results were perpetuated by Schweikert (1915) in a theory which used the results of the Kirchhoff–Helmholtz theory in order to show that they did not apply. The memory of this relatively inaccessible work seems to have been kept alive in cautious footnotes ever since, and lent plausibility no doubt, by the anomalous results of workers who, from time to time, have used cavities whose walls have not been sufficiently polished to make the theory applicable.

The theory of the boundary layer (Fritche 1960; Colclough 1972; Rayleigh 1945) predicts the existence of two wave numbers q_1, q_2 in addition to the wavenumber q of the normal sound wave. The former is associated with thermal loss and the latter with viscous loss. It is found that

$$q_1 \approx (1+\mathrm{i})\left\{\frac{\rho c_p}{K}\frac{\omega}{2}\right\}^{\frac{1}{2}} \approx (1+\mathrm{i})\times 3.2\times 10^2\,\mathrm{cm}^{-1} \tag{18}$$

and

$$q_2 \approx (1+\mathrm{i})\left\{\frac{\omega}{2\nu}\right\}^{\frac{1}{2}} \approx (1+\mathrm{i})\times 3.9\times 10^2\,\mathrm{cm}^{-1} \tag{19}$$

for argon at s.t.p. at a frequency of 5.6 kHz. The imaginary part of these wavenumbers can be shown to constitute a massive absorption coefficient,† the reciprocal of which may be taken as a measure of the boundary layer thickness. This will therefore be of the order of 0.001 cm for argon at s.t.p. Clearly a polished finish is required if the wall is to be taken as smooth with reference to this dimension. Otherwise the usual formulation of the radial boundary condition ceases to be applicable.

In an instrument where changes in frequency can be made there should be no difficulty in principle in checking the orthodox boundary layer theory experimentally – at least insofar as frequency dependence is concerned. But there would remain the problem of evaluating the constant of proportionality between $\alpha_{\mathrm{K.H.}}$ and the square root of the frequency. Experimental measurements of the transport properties of gases are not of sufficient accuracy for our purpose. Fortunately, however, it is possible to measure experimentally the absorption coefficient, $\alpha_{\mathrm{K.H.}}$. As a result, the boundary layer correction can be made by using only a limited set of theoretical relations, i.e. just equation (13) and not equation (14). In fact the assumption underlying equations (12) and (13) is that the complex propagation constant $q = k - \mathrm{i}\alpha$ for the plane wave in the cavity is given by an expression of the form

$$q^2 = q_0^2\{1 + (2\mathrm{i})^{\frac{1}{2}} A\} \approx k_0^2\{1 + (1+\mathrm{i})\, A\}. \tag{20}$$

† These are quoted in the time dependence convention used by Fritche where all quantities vary as $\exp(-\mathrm{i}\omega t)$ which ensures that the waves do decay exponentially given the factor $(1+\mathrm{i})$ in the wavenumber.

Downloaded from rsta.royalsocietypublishing.org

The approximation, k_0, is valid for $q_0 = k_0 - i\alpha_0$ because α_0, the classical absorption coefficient arising from thermal and viscous losses in the body of the gas, is very small ($\alpha_0/k_0 \approx 10^{-5}$ and $\alpha_0/\alpha_{\text{K.H.}} \approx 10^{-2}$). We then obtain directly, by equating real and imaginary parts

$$\frac{k^2 - k_0^2}{k_0^2} = -A = \frac{2k\alpha_{\text{K.H.}}}{k_0^2} \tag{21}$$

and hence equation (12).

In the above relations we had for A

$$A = \frac{1}{b}\left\{\nu^{\frac{1}{2}} + (\gamma - 1)\left(\frac{K}{\rho c_p}\right)^{\frac{1}{2}}\right\}\left\{\frac{\omega}{2}\right\}^{-\frac{1}{2}}. \tag{22}$$

We now see that neither the form of the expression containing the transport coefficients for the gas, nor the frequency dependence need concern us. All that is required is that the factor $(2i)^{\frac{1}{2}}$ should multiply A in equation (20). This may be shown to be the case for any mechanism causing particle velocity to fall to zero at the boundary in accordance with a diffusion equation. And it is the form of this factor that is the minimum theoretical assumption which needs to be made. However, if measured values for A and the observed frequency dependences of $\alpha_{\text{K.H.}}$ and c are as predicted theoretically, it would be very difficult not to conclude that the theory as a whole was reliable.

In applying the above theory another device may be usefully employed to improve the experimental data. All classical loss mechanisms are proportional in some power to the kinematic viscosity or the thermal diffusivity. Since these quantities are inversely proportional to the gas density, we would expect an extrapolated curve of $1/\alpha_{\text{K.H.}}$ against pressure fitted through data taken at practical pressures to pass through the origin. Thus we may take the origin as an exact theoretical point which should help to define the slope of a line fitted to experimental values of $1/\alpha_{\text{K.H.}}$ necessarily measured at higher pressures.

2.3. *The theory of the interferometer*

Since we are proposing to measure wavelength, and hence velocity, to an accuracy of some 2 parts in 10^5 a detailed description is required of the way in which the velocity of sound is derived from the experimental observations obtained with the interferometer. For the purposes of this discussion the interferometer can be considered to consist of a cylinder having one end closed by an electromagnetically driven diaphragm facing a moveable reflector at the other (see figure 4).

It may be shown (Colclough 1972) that the measured complex mechanical impedance† of the transducer, even where it does not vibrate with the same amplitude over the whole of its face, may be written in the form

$$\boldsymbol{Z}(l) = \boldsymbol{Z}_{\text{T}} + \boldsymbol{Z}_{\text{G}}(l), \tag{23}$$

where $\boldsymbol{Z}_{\text{T}}$ is the complex mechanical impedance of the transducer itself and $\boldsymbol{Z}_{\text{G}}(l)$ that due to the gas loading. The latter takes the form

$$Z_{\text{G}}(l) = \pi b^2 \rho c\{R_{\text{G}}(l) - iX_{\text{G}}(l)\}, \tag{24}$$

where

$$R_{\text{G}}(l) = \frac{1 - R_{\text{R}}^2 R_{\text{T}}\, e^{-4\alpha l} + R_{\text{R}}(1 - R_{\text{T}})\, e^{-2\alpha l}\cos 2kl}{1 - 2R_{\text{R}}R_{\text{T}}\, e^{-2\alpha l}\cos 2kl + R_{\text{R}}^2 R_{\text{T}}^2\, e^{-4\alpha l}}, \tag{25}$$

and

$$X_{\text{G}}(l) = \frac{R_{\text{R}}(1 + R_{\text{T}})\, e^{-2\alpha l}\sin 2kl}{1 - 2R_{\text{R}}R_{\text{T}}\, e^{-2\alpha l}\cos 2kl + R_{\text{R}}^2 R_{\text{T}}^2\, e^{-4\alpha l}}, \tag{26}$$

† In this work, for reasons of experimental convenience, the directly measured quantity was admittance (reciprocal impedance). But, as is shown in appendix A, admittance data may be processed in the same way as impedance data.

PHILOSOPHICAL TRANSACTIONS OF THE ROYAL SOCIETY A MATHEMATICAL, PHYSICAL & ENGINEERING SCIENCES

PHILOSOPHICAL TRANSACTIONS OF THE ROYAL SOCIETY A MATHEMATICAL, PHYSICAL & ENGINEERING SCIENCES

Downloaded from rsta.royalsocietypublishing.org

and where R_R and R_T are the reflexion coefficients of the reflector R and the transducer T respectively.† In the work which follows we shall assume that $R_R = R_T = \sigma$. (Since alignment losses are so easily made negligible, we need only consider the boundary layer losses which depend on the transport properties of the gas rather than on peculiarities of the end faces: cf. equation (16).) The phase change, δ, on reflexion has also been ignored in accordance with our choice of a variable path device. Equations (25) and (26) then become

$$R_G(l) = \frac{1-\sigma^3 e^{-4\alpha l}+\sigma(1-\sigma) e^{-2\alpha l}\cos 2kl}{1-2\sigma^2 e^{-2\alpha l}\cos 2kl+\sigma^4 e^{-4\alpha l}}, \tag{27}$$

and

$$X_G(l) = \frac{\sigma(\sigma+1)\sin 2kl}{1-2\sigma^2 e^{-2\alpha l}\cos 2kl+\sigma^4 e^{-4\alpha l}}. \tag{28}$$

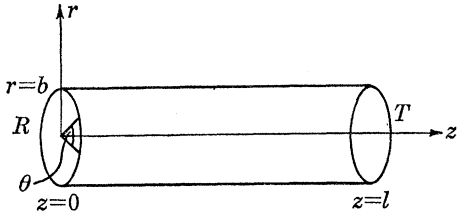

FIGURE 4. The acoustic interferometer cavity.

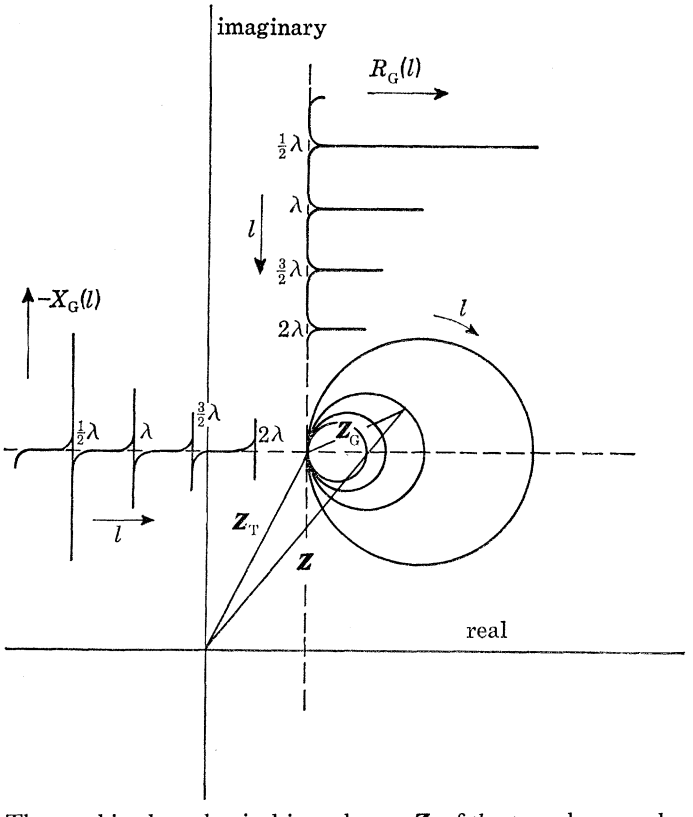

FIGURE 5. The combined mechanical impedance, Z, of the transducer and gas column.

† We have followed common practice in ignoring a factor $\frac{1}{2}(1+R_T)$ in the expressions for $R_G(l)$ and $X_G(l)$. Since it is common to both of them its omission is of no consequence (see appendix B).

Downloaded from rsta.royalsocietypublishing.org

Figure 5 shows the form of the functions $R_G(l)$ and $X_G(l)$ and that the locus of $\mathbf{Z}_G(l)$ is a series of almost perfect circles in the complex plane which are approximately touching when $\mathbf{Z}_G(l) = 0$ if $\beta \equiv 1-\sigma \ll 1$ and $\alpha l \ll 1$. Resonance occurs where $l = N\lambda/2$ ($N = 1, 2, 3, \ldots$) and antiresonance where $l = (2N-1)\lambda/4$. The ratios of the diameters of the circles are shown as being $1 : \frac{1}{2} : \frac{1}{3} : \frac{1}{4} : \ldots$ diminishing as the order of resonance, N, increases. This is characteristic of the situation where reflexion losses are negligible ($\beta \ll \alpha l$). In this case equations (27) and (28) would simplify to give the more familiar equations

$$R_G(l) = \frac{\sinh 2\alpha l}{\cosh 2\alpha l - \cos 2kl} \tag{29}$$

and

$$X_G(l) = \frac{\sin 2kl}{\cosh 2\alpha l - \cos 2kl} \tag{30}$$

for an acoustic interferometer with perfect reflectors.

It is possible to reconstruct the impedance circle diagram of $\mathbf{Z}_T + \mathbf{Z}_G(l)$ as in figure 5 from a direct measurement of the modulus of the combined complex mechanical impedance $\mathbf{Z}(l)$. The techniques have been described by Colclough (1973). However, it is sufficient to assume for our purposes that the circles have been directly plotted with a high quality phase sensitive detection system so that the intrinsic impedance of the transducer, $\mathbf{Z}_T$, can be ignored.

The diameter, D_N, of the Nth circle is given to a very good approximation by $R_G(N\lambda/2)$ (see appendix B). In units of $\pi b^2 \rho c$:

$$R_G(N\lambda/2) = 1/(\alpha l + \beta) \tag{31}$$

which is an appropriate expression for an instrument where β may not be negligible. Thus by fitting a function of the form $1/(aN+b)$ to the experimentally measured diameters, D_N, where $a/b = \alpha\lambda/2\beta$ the ratio α/β may be calculated. In order to evaluate α, a further relation with β is required. This is best obtained by measuring the half width, Δ_N, at half height of the resonances:

$$\Delta_N = (\alpha l + \beta)/k. \tag{32}$$

Δ_N is half the change in l required to traverse the impedance circle from its uppermost point, through resonance, to its lowest point, i.e. one half the separation of the maximum and minimum of $X_G(l)$ close to $N\lambda/2$. Circle diameters are easier to measure than half widths so the preferred approach to evaluating α is to calculate $y = \alpha/\beta$ from a fit to the circle diameters as described and then to substitute it into the expression for Δ_N to give $\alpha = k\Delta_N/(l + 1/y)$. This may then be averaged over the different measured values of Δ_N (one for each resonance) to enable the boundary layer correction to be made.

It is also necessary to find the true position of resonance on the impedance circles so that $N\lambda/2$ and hence the acoustic velocity may be calculated. This is best done by noting the length, l, of the cavity at different phases, ϕ, of the gas impedance $\mathbf{Z}_G(l)$ near resonance. It is shown in appendix B that higher order terms in αl, β and $k(l_N - l)$ may be ignored giving

$$\tan\phi = -\frac{X_G(l)}{R_G(l)} \approx \frac{l_N - l}{\Delta_N} \tag{33}$$

near $l_N = N\lambda/2$. However, the phase ϕ at some point P on the impedance circle is the angle between the line joining antiresonance and P and the main antiresonance–resonance diameter. Given an impedance circle drawn without accurate location of axes, it is only possible to make a rough estimate of the position of antiresonance from the point at which the circle was traversed

Downloaded from rsta.royalsocietypublishing.org

most slowly. We take this as an approximation to antiresonance and measure rough phases, ϕ', with respect to it. Then

$$\tan\phi = \frac{\tan\phi' + \tan\frac{1}{2}\theta}{1 - \tan\phi'\tan\frac{1}{2}\theta} = \frac{l_N - l}{\Delta_N}, \tag{34}$$

where θ is the small angle between the diameters drawn through our estimated antiresonance and the true one. Consequently we may write

$$ax + by + cz = d, \tag{35}$$

where the coefficients may be measured:

$$\left.\begin{aligned} a &= l\tan\phi', \\ b &= \tan\phi', \\ c &= 1, \\ d &= l, \end{aligned}\right\} \tag{36}$$

and the unknown variables are

$$\left.\begin{aligned} x &= \tan\tfrac{1}{2}\theta, \\ y &= -l_N\tan\tfrac{1}{2}\theta - \Delta_N, \\ z &= l_N - \Delta_N\tan\tfrac{1}{2}\theta. \end{aligned}\right\} \tag{37}$$

There are thus three unknown variables x, y and z or l_N, θ and Δ_N so that three values of l and ϕ' have to be measured for each impedance circle. The three resulting simultaneous equations are easily solved for x, y and z to give

$$l_N = \frac{z - xy}{1 + x^2} \tag{38}$$

then

$$\Delta_N = -(y + xl_N). \tag{39}$$

Since $\theta \ll 1$, we have $\theta \approx 2x$ rad.

The above calculations have proceeded on the assumption that the quantities, αl, β and $k(l_N - l)$ are sufficiently small in the neighbourhood of a resonance to allow terms of order two and above in them to be neglected in comparison. In appendix B it is shown that this is a satisfactory assumption giving rise to a change in c_0 of only 10 p.p.m. which can be corrected for subsequently.

3. The practical instrument

A practical interferometer was constructed in accordance with the principles outlined in the previous section and by Colclough (1973) and Quinn (1972). It was designed to be operated at some fixed frequency below its first cut-off frequency and could be brought into resonance by moving an acoustic reflector. The instrument was designed to operate in an ice bath at a temperature as close as possible to 273.16 K, the exact temperature being measured by a calibrated platinum resistance thermometer. Argon was chosen as the experimental gas since it was necessary to be able to determine isotopic composition sufficiently accurately. The high density of argon was desirable from the point of view of minimizing the boundary layer effect ($\propto \rho^{-\frac{1}{2}}$) and maximizing sensitivity ($\propto \rho^{\frac{1}{2}}$ through the specific acoustic impedance, $\rho c = \rho(\gamma p/\rho)^{\frac{1}{2}}$). Moreover, the second acoustic virial coefficient of argon is very small at 273 K so that c is almost independent of pressure thus facilitating the extrapolation of the isotherm to give c_0.

Careful tests have been carried out on the system to ensure that it conforms with all the relevant theoretical assumptions.

Downloaded from rsta.royalsocietypublishing.org

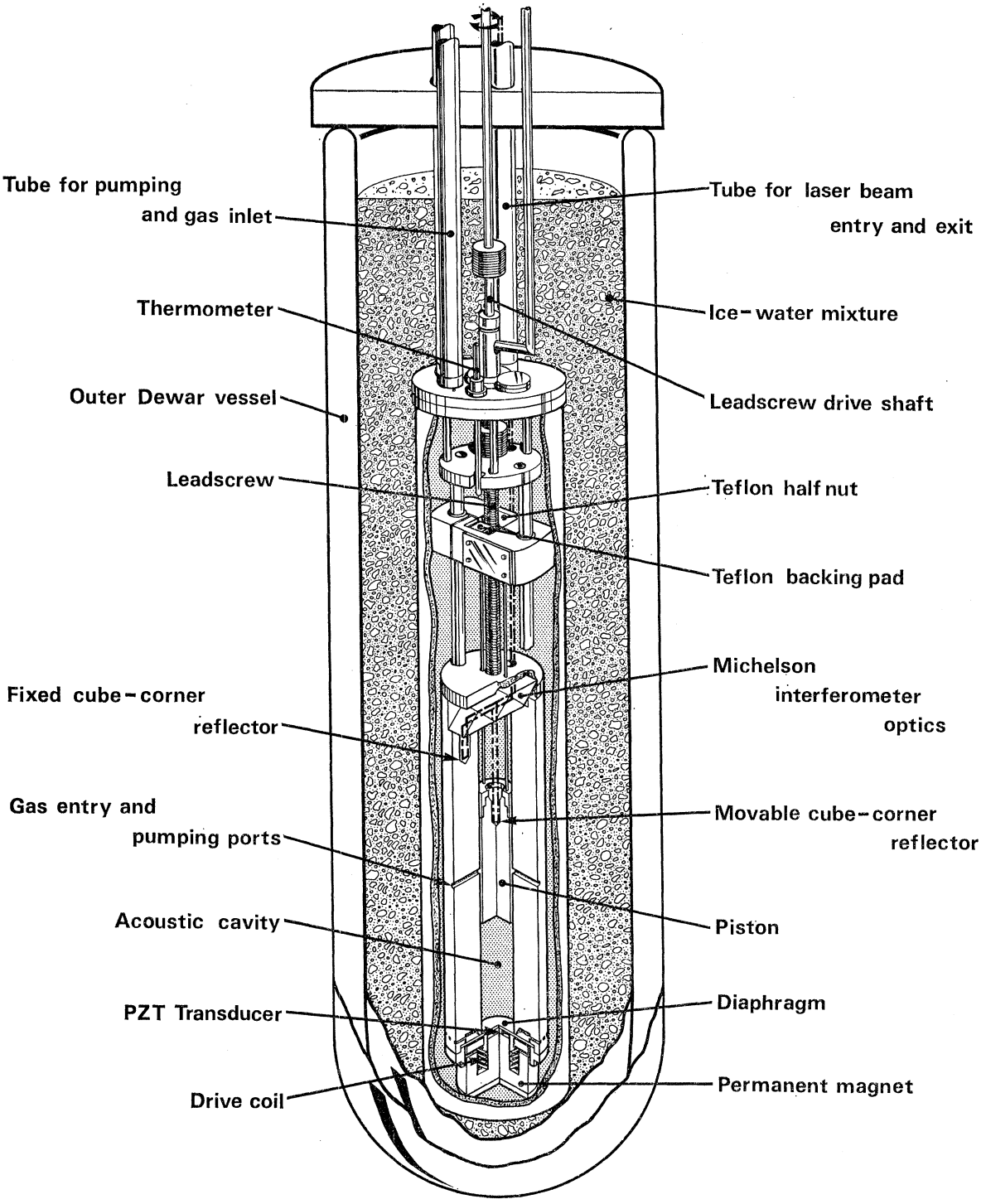

FIGURE 6. The acoustic interferometer, leadscrew mechanism and ice bath.

PHILOSOPHICAL TRANSACTIONS OF THE ROYAL SOCIETY A MATHEMATICAL, PHYSICAL & ENGINEERING SCIENCES

PHILOSOPHICAL TRANSACTIONS OF THE ROYAL SOCIETY A MATHEMATICAL, PHYSICAL & ENGINEERING SCIENCES

Downloaded from rsta.royalsocietypublishing.org

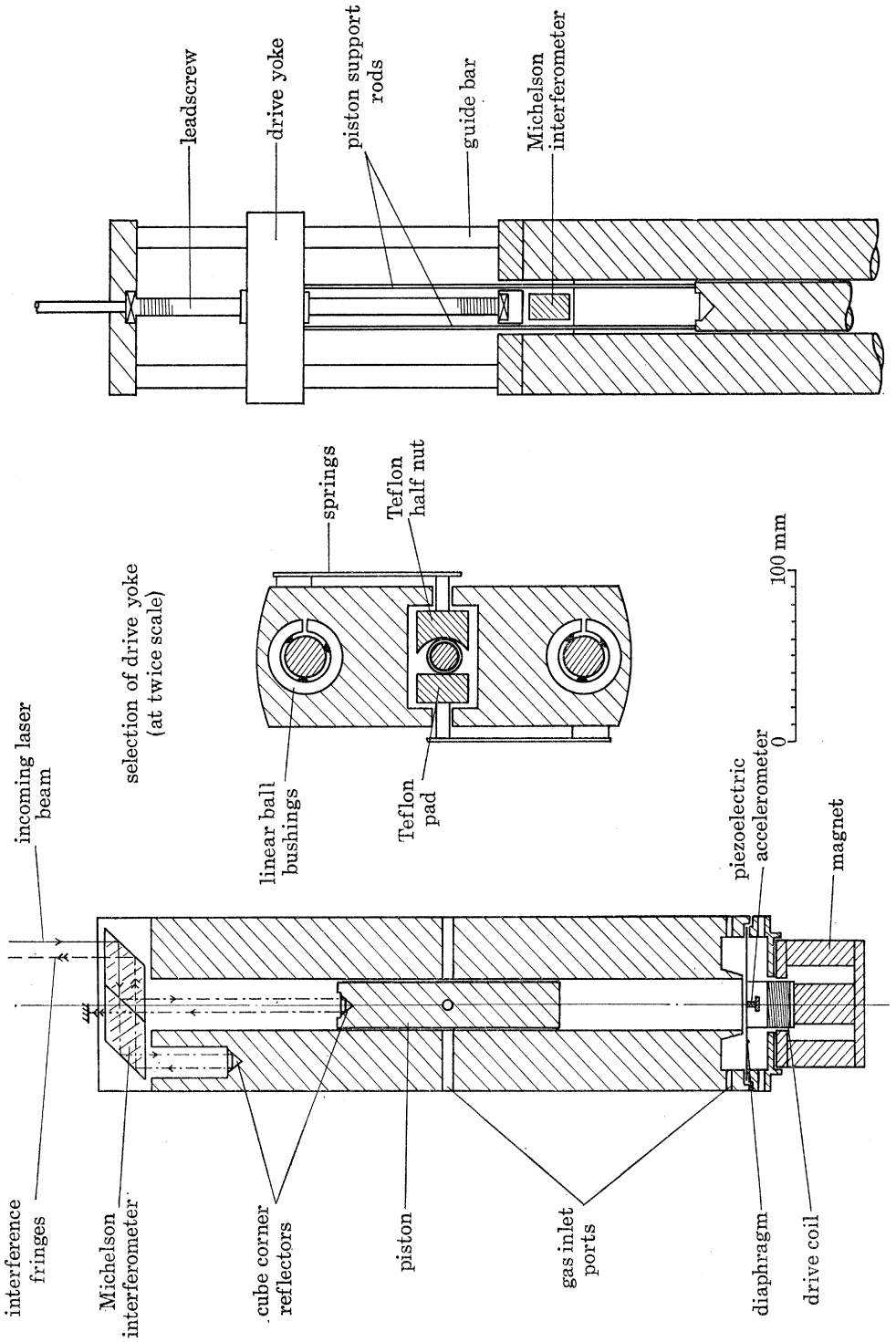

FIGURE 7. Sectional drawing of the interferometer showing the transducer and optical components.

PHILOSOPHICAL TRANSACTIONS OF THE ROYAL SOCIETY A MATHEMATICAL, PHYSICAL & ENGINEERING SCIENCES

PHILOSOPHICAL TRANSACTIONS OF THE ROYAL SOCIETY A MATHEMATICAL, PHYSICAL & ENGINEERING SCIENCES

Downloaded from rsta.royalsocietypublishing.org

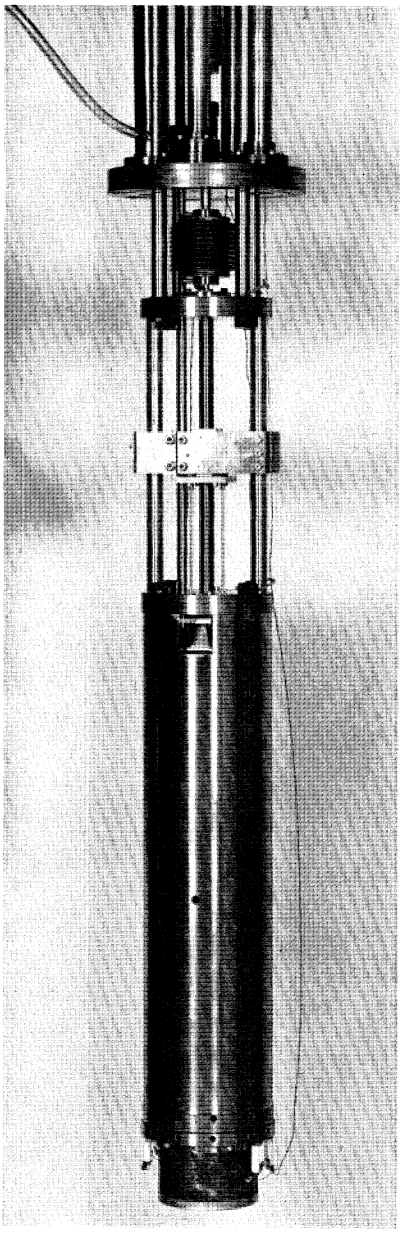

FIGURE 8. The acoustic interferometer assembly.

(*Facing p.* 382)

PHILOSOPHICAL TRANSACTIONS OF THE ROYAL SOCIETY A MATHEMATICAL, PHYSICAL & ENGINEERING SCIENCES

PHILOSOPHICAL TRANSACTIONS OF THE ROYAL SOCIETY A MATHEMATICAL, PHYSICAL & ENGINEERING SCIENCES

Downloaded from rsta.royalsocietypublishing.org

3.1. *The acoustic interferometer*

The acoustic interferometer is shown in figures 6, 7, figure 8, plate 1 and figure 9 suspended in its canister which also houses the leadscrew mechanism for raising and lowering the piston whose lower face functions as the acoustic reflector. The whole instrument is in an argon atmosphere which, being at constant volume and almost wholly at constant temperature,

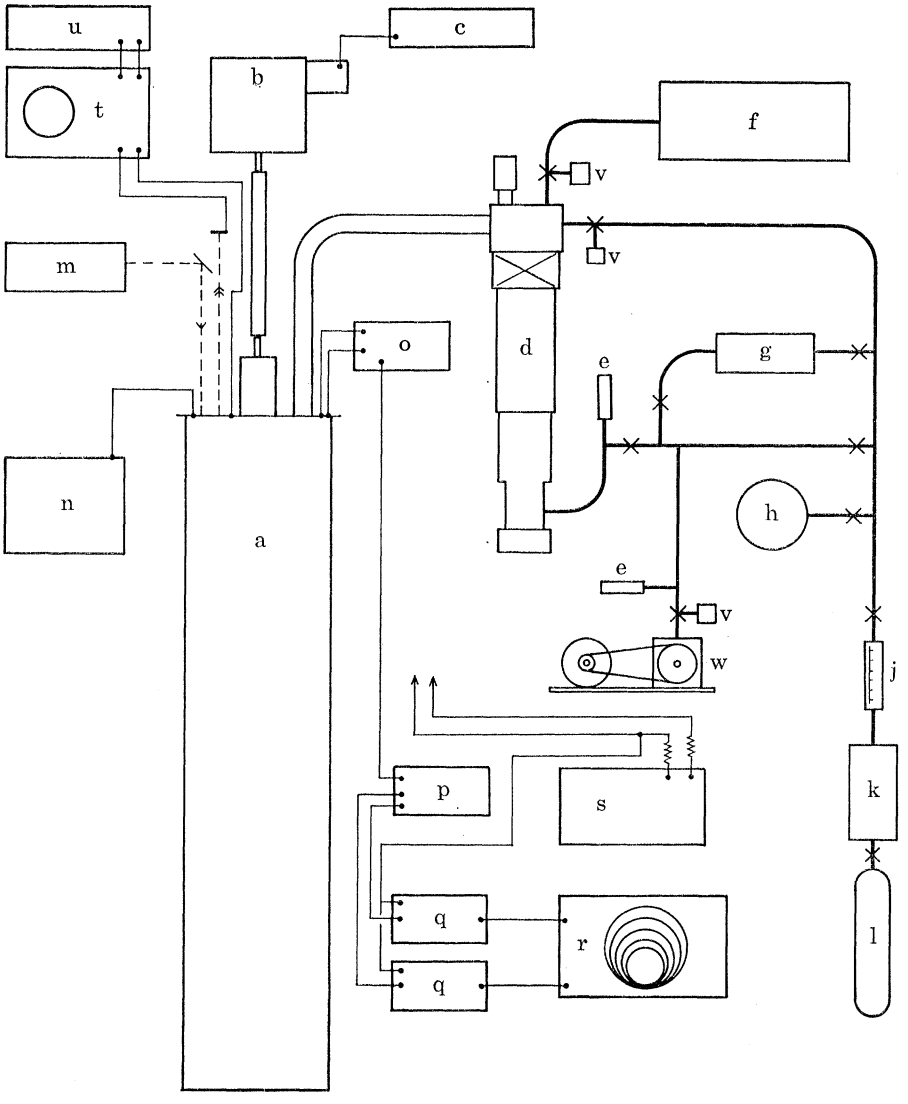

a acoustic interferometer
b piston drive unit
c remote control for *b*
d diffusion pump and cold trap
e vacuum gauges
f mass spectrometer
g quartz spiral pressure gauge
h precision dial type pressure gauge
j argon flow meter
k argon purifier
l argon storage cylinder
m laser
n measuring bridge for resistance thermometer
o high input impedance amplifier for PZT accelerometer
p phase splitter unit
q phase sensitive detector units
r *X*–*Y* plotter
s frequency synthesizer
t oscilloscope and photocell amplifiers
u reversible counter
v solenoid vacuum valves
w rotary pump

FIGURE 9. Block diagram of the gas handling and electronic systems.

Downloaded from rsta.royalsocietypublishing.org

requires no pressure controlling system. It is this argon which fills the acoustic cavity so that for the purpose of purity control all the components in the canister were designed to be bakeable under vacuum at 100 °C to lower their subsequent outgassing rate to an acceptable level. The canister itself hangs in an ice bath and the interferometer carries a platinum resistance thermometer† calibrated in a triple point cell.

The transducer which excites the cavity and monitors the resonances is a moving coil driven 'Duralumin' diaphragm of 0.025 cm thickness clamped at the mouth of the cavity facing the moving reflector. It had been carefully annealed between lapped steel blocks. On its rear face it carries a small lead zirconate titanate (PZT) synthetic piezoelectric accelerometer whose function will be explained in greater detail below.

On the upper end of the piston is located an optical cube-corner reflector which constitutes the moving mirror of a Michelson interferometer. At the top of the bore in which the piston slides is placed a glass block containing a beam splitter and two 45° mirrors. The first mirror diverts the laser beam coming from outside the apparatus onto the beam splitter and returns interfering beams. The second, in the opposite side of the block, enables the Michelson's fixed arm to be bent so that it can be accommodated more easily in the canister. The Michelson interferometer works either side of zero path difference which allows a comparatively short and cheap laser to be used. A He–Ne laser with a 27 cm cavity and a power rating of 1 mW was employed with conventional photocells and d.c. amplifiers. The wavelength in vacuum of the laser light was taken as 632.99141 nm and the wavelength in argon at pressure p was calculated from the simple expression

$$632.99141\ (1 - 0.000281\, p/P_0)\ \text{nm},$$

where p/P_0 is the pressure in standard atmospheres and 1.000281 is the refractive index of argon at n.t.p. A quadrature output from the Michelson interferometer enables a bi-directional counter to be used so that reversing the piston's motion caused no problems whether done intentionally or by any unexpected mechanical disturbance. The frequency response of this fringe counting system extended to 1 MHz to reduce the risk of fringes being lost in the event of sudden jolts. Care was taken in the alignment of the optical interferometer so that it measured truly axial piston displacements. This ensured that the corresponding cosine error was less than 3 p.p.m.

The first acoustic cut-off wavelength is given by

$$\Lambda_{10} = \frac{2\pi b}{X_{10}} = 3.42b, \tag{40}$$

where b is the cavity radius and $X_{10} = 1.84$ is a number characterizing the first solution of the radial boundary condition (Colclough 1972, 1973). Thus, having decided to work below the first cut-off frequency, we are obliged to use wavelengths greater than 3.42 cavity radii. It was decided, somewhat arbitrarily, that a little over five half wavelengths should be a sufficient length for the fully extended cavity giving three more than the absolute minimum of two required to calculate α and β. Should any unexpected systematic deviation of resonance separation with acoustic path occur, it would be likely to be greatest in the early orders of resonance where $l \approx \lambda$. By the fifth order it might be expected to show a change and thus betray its presence. To keep the cavity as short as possible, thus facilitating temperature control, it was desirable to use a bore of

† The working temperature of the acoustic interferometer will not be exactly 273.16 K and so a knowledge of the resistance/temperature derivative of the platinum resistance thermometer will be required so that small corrections can be made to the velocity. But as pointed out in § 1 prior knowledge of the gas constant is not in principle required to make this calibration.

Downloaded from rsta.royalsocietypublishing.org

small radius (cf. equation (40)). On the other hand, boundary layer errors would then increase and the loading of the gas column on the transducer would decrease so leading to a drop in sensitivity. A value of $b = 1.5$ cm was finally chosen by way of compromise which just enabled the small cube-corner to be comfortably accommodated on top of the piston while still leaving room for the two piston support rods either side which move it. This gave a value of 5.13 cm for Λ_{10}, a corresponding cut-off frequency $f_{10} = 6$ kHz and a traverse of 13 cm when operated at a frequency $f = f_{10}$. In practice, it is necessary to allow a little extra traverse so that the operating frequency can be taken a little way below the first cut-off frequency to a point where the first higher mode is well and truly cut off, and where there is a little latitude in the choice of operating frequency so that any unfortunate resonance in the transducer can be avoided. In our instrument it was found that $\boldsymbol{Z}_{\mathrm{T}}$ was small and stable around 5.600 kHz and this was the chosen operating frequency. The total piston traverse available was 15.3 cm of which approximately 14 cm were used. When the piston was fully raised four pumping ports were exposed to facilitate outgassing.

Both piston and cavity were made of brass, the latter being plated to a thickness of about 0.005 cm with nickel-tin by the Tin Research Institute. This forms a hard, easily lapped finish which is suitable for high vacuum surfaces and which can be applied evenly in a long narrow bore. The piston was not so plated in accordance with the belief that dissimilar surfaces are less likely to wring together when in very close contact. This was felt to be a real risk with the fine tolerances to which the piston and cylinder were finally lapped together.

Investigations were carried out so that the mechanical alignment of the reflecting piston face, the bore and the transducer could be assessed. The cavity was laid horizontally in two 'v' blocks and a glass plate, aluminized except for a circular window looking into the mouth of the cavity, was held against the surfaces on which the transducer diaphragm was normally located. An autocollimator was then used to compare the alignment of the aluminized glass plate and the piston face at various positions in the cavity by comparing the separations of crosswire images returned from the two surfaces. It was found that the angular misalignment was never larger than 50″ (seconds of arc) or 2.4×10^{-4} rad which was, for our purposes, entirely negligible. The squareness of the piston face to the cavity axis was also checked at several positions in the bore by rotating the piston through 180° and measuring the resulting angular displacement from the change in position of its crosswire image. It was possible to check that no cavity movement occurred during this operation from the position of the crosswire image from the glass plate. The estimated angular misalignment of the piston face was never greater than 10″ or 5×10^{-5} rad – again, an entirely negligible amount.

In order to measure the phases, ϕ, of the gas loading $\boldsymbol{Z}_{\mathrm{G}}(l)$ for various values of l, a high quality phase sensitive detection (p.s.d.) system was employed (see figure 9). The most critical unit was a phase splitter (type 422) supplied by Brookdeal Electronics Ltd, which provided an accurate in-phase and quadrature output from an input signal. The two outputs were then used as reference signals for two phase sensitive detectors from the same manufacturer. The signal fed to this system came from the PZT accelerometer via a high input impedance differential amplifier (Brookdeal type 432) and the reference voltage was taken from across a resistor in series with the driving coil. Thus the outputs of the system correspond to the in-phase and quadrature components of transducer velocity with respect to driving force (if we ignore a factor $i\omega$ which is constant at constant frequency). The mechanical impedance $\boldsymbol{Z}(l) = \boldsymbol{Z}_{\mathrm{T}} + \boldsymbol{Z}_{\mathrm{G}}(l)$ is measured in arbitrary units by the reciprocal of the transducer velocity at constant driving force (i.e. constant current in our moving coil device) and so, by feeding both phase sensitive detector outputs to an X–Y

PHILOSOPHICAL TRANSACTIONS OF THE ROYAL SOCIETY A MATHEMATICAL, PHYSICAL & ENGINEERING SCIENCES
PHILOSOPHICAL TRANSACTIONS OF THE ROYAL SOCIETY A MATHEMATICAL, PHYSICAL & ENGINEERING SCIENCES

Downloaded from rsta.royalsocietypublishing.org

recorder, *admittance* circles can be plotted as the piston is raised through successive resonances. These circles may be processed as described in the previous section (see appendix A). Antiresonance is now at $\boldsymbol{Z}_{\mathrm{T}}^{-1} = \boldsymbol{Z}_{\mathrm{T}}^{*}/Z_{\mathrm{T}}^{2}$ in the complex plane and generally the circles are defined by $\boldsymbol{Z}^{-1}(l) = \boldsymbol{Z}^{*}(l)/Z^{2}(l)$. The reason for using an accelerometer rather than measuring the gas loading conventionally through its effect on the electrical impedance of the transducer, was that in the latter method $\boldsymbol{Z}_{\mathrm{T}}$ is increased relative to $\boldsymbol{Z}_{\mathrm{G}}(l)$ by the purely electrical component of the transducer impedance whereas in the accelerometer method the coil impedance is not included and mechanical impedances are measured directly. It is important to keep $\boldsymbol{Z}_{\mathrm{T}}$ as low as possible since, at very low pressures, $\boldsymbol{Z}_{\mathrm{G}}(l)$ decreases and becomes masked by $\boldsymbol{Z}_{\mathrm{T}}$ so that the instrument becomes insensitive. Increased amplification of the PZT signal is of no use beyond the point at which it overloads the p.s.d. system at antiresonance. It is this mechanism which prevents us from measuring sound velocities at sufficiently low pressures to make the effect of the virial coefficients negligible. But it is important, nevertheless, to minimize the range of extrapolation to zero pressure if the isotherm intercept is to be well defined. So for this reason the accelerometer method is to be preferred.

3.2. *Chemical and isotopic analysis of argon*

Both the chemical purity and the isotopic composition of the gas had to be considered in detail. The argon chosen for the experiment was supplied by the British Oxygen Company (B.O.C.) in a steel cylinder containing 8.5 $\mathrm{m^3}$ (300 $\mathrm{ft^3}$) initially under a pressure of 17 MPa (2500 $\mathrm{lbf/in^2}$). Chemical purity was achieved by using a commercial chemical system (B.O.C. inert gas purifier) which absorbed all impurities except helium down to the level of a few parts per million. Most of the residual impurities found in the argon during operation were shown to be the result of desorption of gas in the system. The arrangement of the gas handling equipment is shown in figure 9. The mass spectrometer (VG Micromass type M52), purifier and pressure gauge were arranged so that the whole of the pipework connecting them to the main chamber of the interferometer could be heated to 150 °C by the passage of an electric current of 200 A. The main chamber of the acoustic interferometer was heated to 75 °C by means of an external heating tape and kept at this temperature for 72 h.

After mass spectrometer leak testing and baking out the residual pressure measured by the ionization gauge fell to *ca.* 90 μPa (7×10^{-7} Torr). The only impurity species detectable with the mass spectrometer were nitrogen and water vapour. Typical analyses in one atmosphere of argon indicated 14 p.p.m. of nitrogen and 2 p.p.m. of water vapour. It was found that in one day's operation of the system, during which as many as ten sets of impedance circles would be taken, the background level of nitrogen did not rise to more than 20 p.p.m. even at the lowest pressures. Since the velocity of sound in nitrogen is greater than that in argon by only 9 % the effect on the measured velocity in argon of the presence of 10 p.p.m. of nitrogen amounts to only 2 p.p.m. Nevertheless it was the practice to change the argon for a fresh filling at the end of each day's work so that by the following morning temperature equilibrium would have been reached.

The measurement of the isotopic composition of the sample used for this work posed considerable problems. The information available on the likely variation in isotopic content of argon is sparse. The recent work of Melton, Massey & Abels (1971) on the isotopic composition of natural argon gives

$$^{40}\mathrm{Ar} = 99.597\ \%,$$
$$^{38}\mathrm{Ar} = 0.064\ \%,$$
$$^{36}\mathrm{Ar} = 0.339\ \%.$$

Downloaded from rsta.royalsocietypublishing.org

Taking the atomic masses of each isotope to be

$$^{40}\mathrm{Ar} = 39.9624\,\mathrm{g/mol},$$

$$^{38}\mathrm{Ar} = 37.9627\,\mathrm{g/mol},$$

$$^{36}\mathrm{Ar} = 35.9675\,\mathrm{g/mol},$$

from Mattauch, Wapstra & König (1962), we find a molecular mass for natural argon of 39.9476 g/mol. This is very close to the value of 39.9477 g/mol published by Nier (1950). We take the good agreement between the two as indicative of the relatively small differences likely to be found between different samples of natural argon. The constancy of the isotopic composition between samples of argon from different sources is further confirmed by some investigations carried out on our behalf at the Bureau Central de Mesures Nucleaires (B.C.M.N.) at Geel in Belgium.

B.C.M.N. made measurements of the relative isotopic composition of three samples of argon. One was a sample taken from the cylinder used in our work on the gas constant, sample N.P.L./B.O.C.; another was of argon supplied to the B.C.M.N. by Air Liquide, sample B.C.M.N./A.L.; and the third was from argon obtained at the B.C.M.N. by the chemical removal of nitrogen, oxygen and water, etc. from air, sample B.C.M.N./chem.

The results obtained were as follows:

$$\frac{(36/40)_{\mathrm{B.C.M.N./chem.}}}{(36/40)_{\mathrm{B.C.M.N./A.L.}}} = 1.003\,63 \pm 0.000\,17,$$

$$\frac{(36/40)_{\mathrm{B.C.M.N./A.L.}}}{(36/40)_{\mathrm{N.P.L./B.O.C.}}} = 1.001\,95 \pm 0.000\,13,$$

from which we deduce

$$\frac{(36/40)_{\mathrm{N.P.L./B.O.C.}}}{(36/40)_{\mathrm{B.C.M.N./chem.}}} = 0.994\,44 \pm 0.000\,30.$$

Also

$$(38/36) = 0.189,$$

where $(36/40)_{\mathrm{B.C.M.N./chem.}}$ refers to the ratio of the ^{36}Ar to ^{40}Ar for sample B.C.M.N./chem. and similarly for samples B.C.M.N./A.L. and N.P.L./B.O.C. The determination of the (38/36) ratio to the required accuracy was a relatively simple matter.

If we take the isotopic composition of the sample chemically prepared at B.C.M.N. to be that of natural argon, having the composition given by Melton *et al.* (1961) then that of the B.O.C. argon used for the present work can be deduced as follows:

$$^{40}\mathrm{Ar} = 99.598\,\%,$$

$$^{38}\mathrm{Ar} = 0.064\,\%,$$

$$^{36}\mathrm{Ar} = 0.338\,\%.$$

This leads to a molecular mass of 39.9476 g/mol. If, on the other hand, the results of Nier are chosen as representing the isotopic composition of natural argon then we find a molecular mass of 39.9477 g/mol for our argon. The molecular mass of the 'Air Liquide' sample B.C.M.N./A.L., on the basis of the results of Melton *et al.* for natural argon, appears to be 39.9475 g/mol or 39.9476 g/mol following Nier.

In view of the uncertainty which exists as to the relation between the natural argon obtained at B.C.M.N. and the argon used by both Nier and Melton *et al.* we have chosen a molecular mass

Downloaded from rsta.royalsocietypublishing.org

of 39.9476 g/mol. The estimated uncertainty in M based upon the uncertainty of 0.0003 given by B.C.M.N. for the comparison measurements is negligible. We have, therefore, taken the overall uncertainty to be 0.0002 g/mol to encompass the isotopic composition of all the samples. This leads to an overall uncertainty of 5 p.p.m. in R.

3.3. *Temperature pressure and frequency measurement*

The temperature of the acoustic cavity was deduced from measurements made by a Tinsley capsule type platinum resistance thermometer calibrated at the triple point of water and the steam point. The thermometer was suspended by its lead wires and immersed in oil in a thin walled stainless steel tube tightly held in a groove in the outer wall of the interferometer cylinder. Measurements of resistance were made by using an a.c. bridge of the Hill & Miller design.

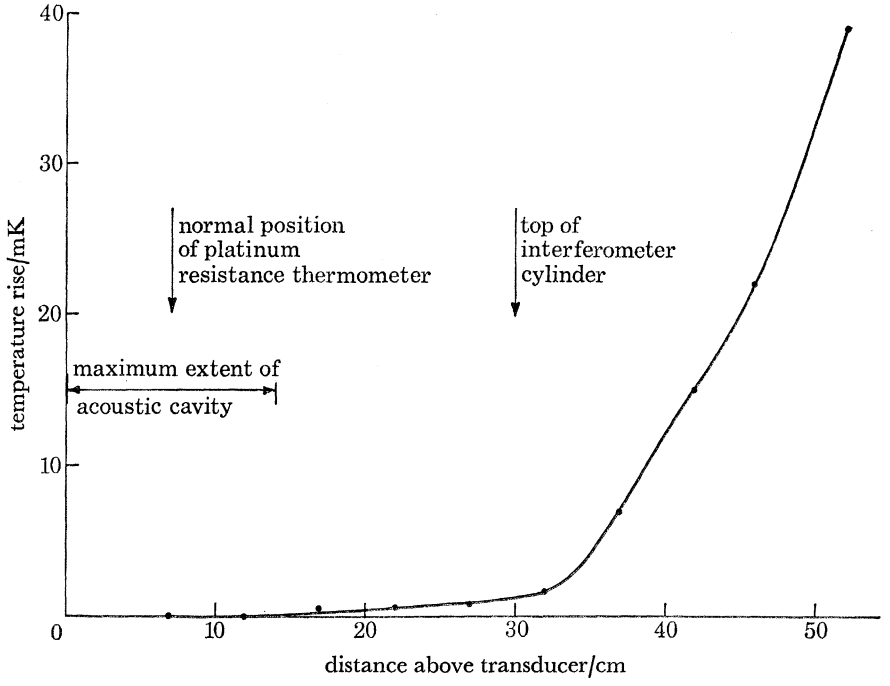

FIGURE 10. The temperature distribution in the instrument.

The temperature distribution upwards from the bottom of the brass cylinder is shown in figure 10. During the measurements of sound velocity the platinum capsule was periodically removed from the acoustic interferometer for re-calibration in a triple point cell. No deviation greater than 0.2 mK was observed. During measurements the temperature was recorded before and after each set of resonance curves and a correction to the calculated sound velocity was made to refer it to 273.16 K. The error in making these corrections is negligible since the temperatures recorded were generally within 10 mK of the triple point and never departed by more than 20 mK.

Pressures were measured by means of a Texas Instruments quartz spiral pressure gauge having a capsule of range 0–300 kPa (3 atm). In view of the very small change of sound velocity in argon with pressure at a temperature of 273.15 K, the requirements for pressure measurement were easily met. A change of 10 kPa (0.1 atm) between 30 and 200 kPa resulted in a change of sound velocity of only about 10 p.p.m.

Downloaded from rsta.royalsocietypublishing.org

The operating frequency of the transducer was another quantity where the requirements for accuracy were easily met. The transducer was driven by a Solartron–Schlumberger type FS 1 digital signal generator. The frequency was found to be in error by less than 2 parts in 10^8. The harmonic distortion was stated to be less than 1 %. We estimate that the acoustic power dissipated was of the order of 1 μW.

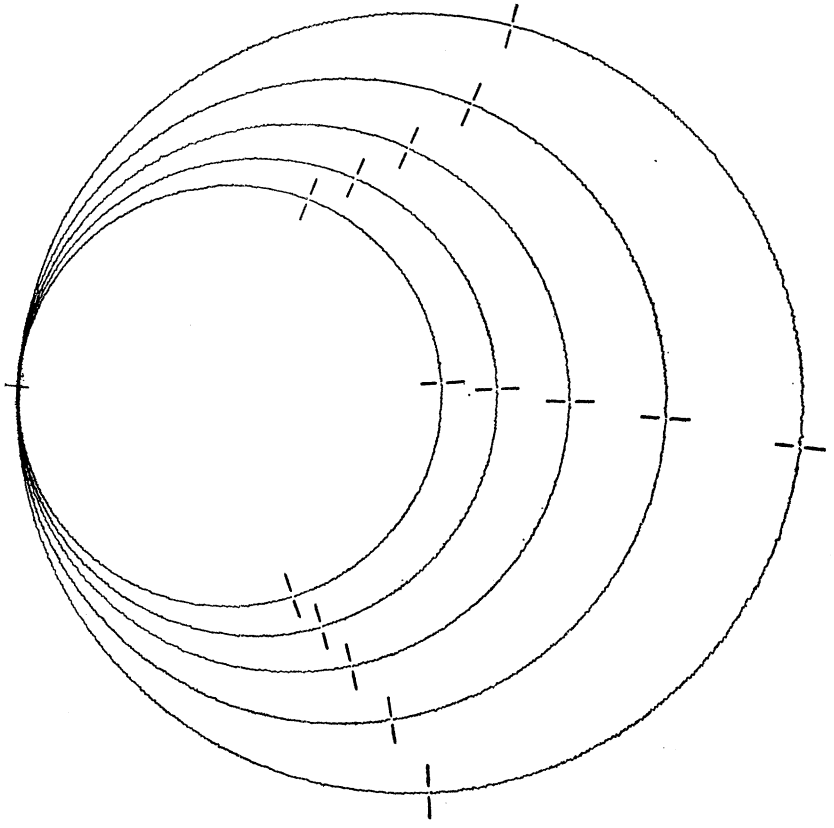

FIGURE 11. A series of five acoustic resonances taken at a pressure of 100 kPa. The original diameter of the largest circle was 200 mm. Points are marked at which the piston was stopped for ϕ and l to be measured.

4. EXPERIMENTAL PROCEDURES AND SYSTEM TESTS

4.1. *General experimental procedure*

For each acoustic isotherm point the cavity was traversed once by the reflector, all five resonances being scanned. A typical set of resonances taken at a pressure of 100 kPa is shown in figure 11. The temperature of the interferometer and the argon was measured just before the first and just after the last resonances were traversed to enable their positions to be corrected to their exact triple point values. Such a correction was always made, but was usually very small. During a traverse which typically took half an hour a smooth increase in temperature of about 1 mK was generally observed. This increase could be unambiguously attributed to mechanical friction in the piston and lead screw mechanism and was not caused by acoustic dissipation. On the contrary, the temperature was observed to fall slowly when the transducer was driven and the piston held stationary. Pressure was also measured at the beginning and end of each traverse.

In order to obtain the three values of Δ_N, $\tan\phi$ and l_N for each resonance, the piston was stopped at three points on each admittance circle (see figure 11). The colour of the X–Y recorder pen was

Downloaded from rsta.royalsocietypublishing.org

changed and the length of the cavity recorded in terms of the optical fringe count. The three points corresponded very roughly to phases of $+45°$, 0, $-45°$. Subsequently, the circle plots were transferred to a calibrated X–Y reader which recorded on punched tape the coordinates of the points where the colour changed and the coordinates of the estimated antiresonant point. A computer program then processed the information as described in § 2 in terms of the coordinate geometry of the circles having first constructed perfect circles through the three stationary points. The phases ϕ' were measured with respect to an antiresonance–resonance diameter put through the centre of these perfect circles and the estimated point of antiresonance of the experimental circles. Since this part of the circle is traversed very slowly, the experimental antiresonance point was also an effectively stationary point. Thus no errors due to the response time of the X–Y recorder can arise in our value of the gas constant.

4.2. *Tests on the form of the circles*

The circles were of high quality (figure 11) and could be shown to possess all the properties attributed to them by the theory. In particular the reciprocal diameters $(1/D_N)$ of the circles constructed through the stationary points at $\phi \doteq 45°$, 0 and $-45°$ were of the form $aN+b$ as were the half widths, Δ_N, calculated from the measurement of ϕ' and l at the three points. In calculating Δ_N it was found necessary to take into account a difference in gain, found to be $1.71\,\% \pm 0.06\,\%$, between the X and Y channels of the phase sensitive detectors and X–Y plotter. Following an initial misalignment the gain on the X-channel was slightly larger than that of the Y-channel. The result was that the main anti-resonance–resonance diameter of all the circles (which always lay closely parallel to the Y-axis) was slightly smaller than the corresponding 'imaginary diameters' (parallel to the X-axis). Each measured value of $\tan\phi'$ had, therefore, to be decreased by 1.71 % leading to increases of 1.71 % in the half widths, absorption coefficient and boundary layer correction. Because of the symmetry of the circles about the Y-axis no corresponding error arises in the measured position of the resonances. The uncertainty in the final value for c_0^2 and hence in R arising from the uncertainty in applying the correction for misalignment of gain is less than 4 p.p.m. No additional departure from circularity in the observed circles is to be expected on the basis of the acoustic theory (appendix B).

Taking a typical set of resonances plotted at one atmosphere pressure we find an angular resolution on the first resonance of about 2.5×10^{-3} rad. This is based upon a resolution of 0.5 mm (approximately equal to the thickness of the recorder trace) on the circumference of a 200 mm diameter circle. On the fifth resonance the corresponding figure is about 5×10^{-3} rad. These angular uncertainties are equivalent to distances of 5×10^{-5} and 1.6×10^{-4} cm respectively. Taking into account the fact that on each circle three such independent measurements are made the overall uncertainties in the position of the first and last resonance peaks are 8.7×10^{-5} cm and 2.8×10^{-4} cm obtained by combining the above figures in quadrature for each circle. This represents a total fractional error in the measurement of wavelengths of 27 p.p.m. This is in good agreement with our final results in which the standard error of the fit of our 98 measurements of velocity about a smooth curve is 36 p.p.m. (see table 5).

In figures 12 and 13 we show plots of $1/D_N$ and Δ_N against the order of resonance, N, taken at approximately 30 and 200 kPa pressure. These pressures represent the lower and upper limits of the isotherm points and indicate the reliability of the theory over the whole range of use of the instrument. The slightly increased scatter at the lower pressure is attributed to the loss of sensitivity arising from the decreased loading of the transducer. In figure 14 a plot of $\tan\phi$ against l

Downloaded from rsta.royalsocietypublishing.org

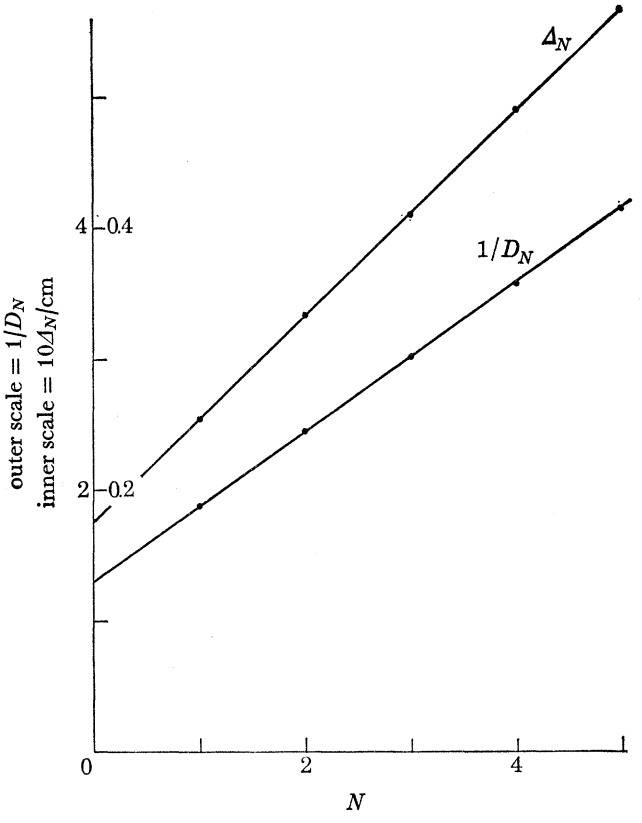

FIGURE 12. Reciprocal circle diameters and halfwidths of resonances plotted against order of resonance at a pressure of 30 kPa. ●, Experimental points.

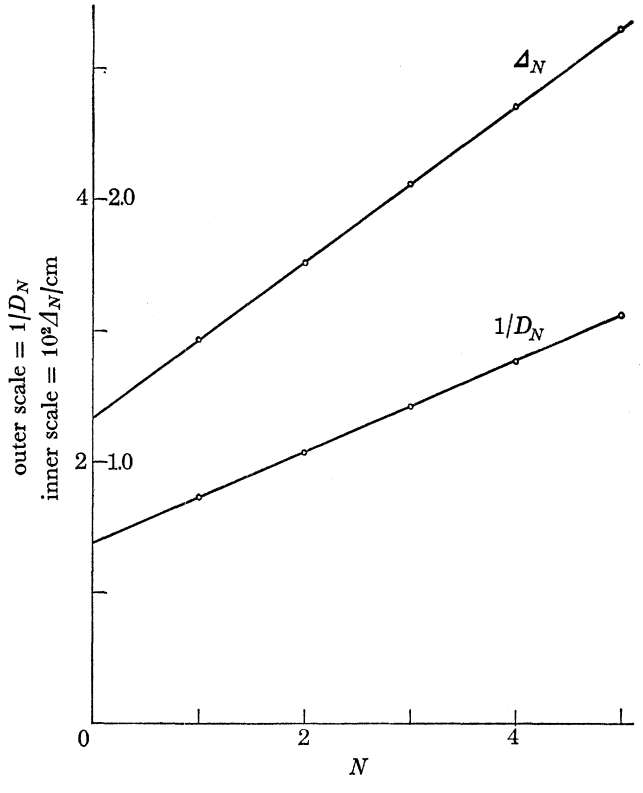

FIGURE 13. Reciprocal circle diameters and halfwidths of resonances plotted against order of resonance at a pressure of 200 kPa.

Downloaded from rsta.royalsocietypublishing.org

is shown. This was obtained by taking the first resonance at approximately 100 kPa and recording many phases and fringe counts as the circle was traversed. The plot can be seen to be linear over that region of the circle where measurements were made thus justifying the fundamental theoretical assumption that $\tan\phi = (l_N - l)/\Delta_N$ where $l_N = N\lambda/2$ and Δ_N, the constant of proportionality, is, by definition, the half width when $\tan\phi = 1$.

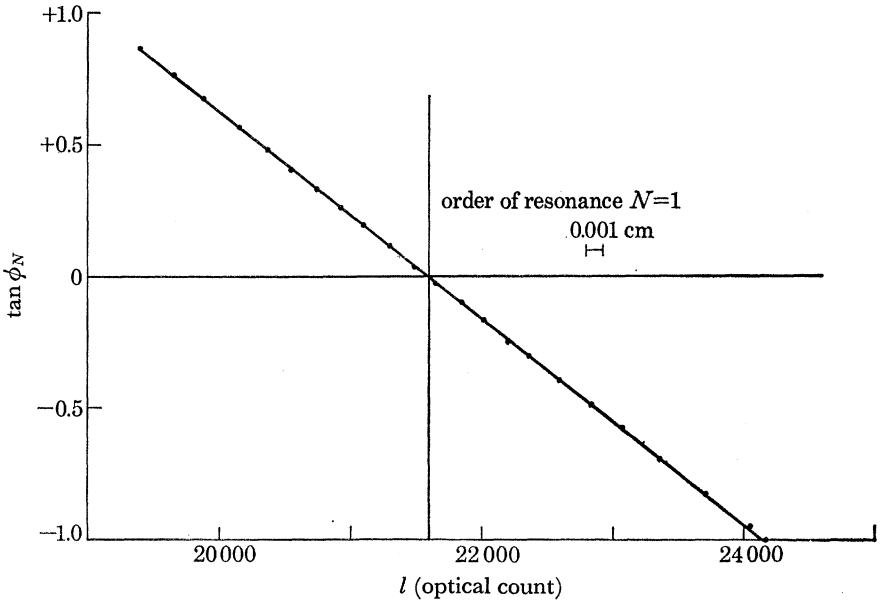

FIGURE 14. The tangent of the phase of the gas impedance as a funtion of cavity length at a pressure of 100 kPa.

4.3. *Boundary layer tests*

Careful tests were made at 10 and 200 kPa to ensure that our principal systematic error – that due to the acoustic boundary layer – could be properly assessed (see tables 1 and 2).

Firstly, the frequency dependence of the boundary layer absorption coefficient, $\alpha_{\text{K.H.}}$ was investigated by taking measurements at four frequencies corresponding to 2, 3, 4 and 5 resonances in the cavity. Tests were limited to this range because at least two resonances had to be accommodated to enable a measurement to be made and because more than five would have entailed raising the operating frequency above the first cut-off frequency.

A calculated value of the classical absorption coefficient, α_0, was subtracted from the measured absorption coefficient, α, to give $\alpha_{\text{K.H.}}$. Since $\alpha_0 \ll \alpha_{\text{K.H.}}$ no significant errors are introduced into $\alpha_{\text{K.H.}}$ by using the conventional formula for α_0

$$\alpha_0 = \frac{1}{2c^3}\left\{\tfrac{4}{3}\nu + (\gamma+1)\frac{k}{\rho c_p}\right\}\omega^2 \tag{41}$$

and the approximate values from table 3 for the quantities appearing therein. It was then assumed that

$$\alpha_{\text{K.H.}} = \frac{A\pi^{\frac{1}{2}}}{bc_0} f^s \tag{42}$$

so that

$$\lg \alpha_{\text{K.H.}} = \lg\left(\frac{A\pi^{\frac{1}{2}}}{bc_0}\right) + s \lg f. \tag{43}$$

Downloaded from rsta.royalsocietypublishing.org

TABLE 1. VELOCITIES AND ABSORPTION COEFFICIENTS AS A FUNCTION OF FREQUENCY AT A PRESSURE OF 10 kPa

f/Hz	$10^3 \alpha_{\text{K.H.}}$/cm^{-1}	c/(m s^{-1}) (measured)
1950	3.764	305.274
1950	3.564	305.200
1950	2.960	305.818
3000	4.737	305.657
3000	3.817	306.043
3000	5.211	304.799
3950	5.480	306.310
3950	4.660	305.939
5600	6.067	305.799
5600	5.980	306.418
5600	5.518	306.511

TABLE 2. VELOCITIES AND ABSORPTION COEFFICIENTS AS A FUNCTION OF FREQUENCY AT A PRESSURE OF 200 kPa

f/Hz	$10^3 \alpha_{\text{K.H.}}$/cm^{-1}	c/(m s^{-1}) (measured)
1950	0.748	307.369
1950	0.753	307.541
1960	0.775	307.525
1970	0.713	307.500
1970	0.748	307.448
1980	0.728	307.561
3000	1.040	307.500
3000	1.107	307.612
3000	1.111	307.643
3950	1.052	307.650
3950	1.030	307.686
3950	1.034	307.655
3950	1.065	307.672
5600	1.231	307.838
5600	1.229	307.753
5600	1.216	307.750
5600	1.234	307.755
5600	1.220	307.770
5600	1.244	307.757

TABLE 3. TRANSPORT PROPERTIES OF ARGON AT 273.16 K

The following values have been used to calculate the acoustic quantities appearing in the text.

$c = 3.078 \times 10^2\ \text{m s}^{-1}$
$\gamma \approx 1.6706$
$K = 1.6454 \times 10^{-2}\ \text{W m}^{-1}\ \text{K}^{-1}$
$\eta = 2.1005 \times 10^{-5}\ \text{N s m}^{-2}$
$c_p = 5.218\ \text{J kg}^{-1}\ \text{K}^{-1}$
$\rho = 1.78382\ \text{kg m}^{-3}$ at n.t.p. (and pro rata at other pressures)
$\omega = 2\pi f$ Hz, $f = 1.95$–5.6 kHz
$\alpha_{\text{K.H.}} = 0.1796\ \text{m}^{-1}$ at n.t.p.
$\alpha_0 = 5.8 \times 10^{-4}\ \text{m}^{-1}$ at n.t.p.

Values of γ, k, η, c_p and ρ are n.t.p. values taken from an assessment of selected data in U.S.B.M. (1967)
γ, k, η and c_p vary only slightly with pressure.

PHILOSOPHICAL TRANSACTIONS OF THE ROYAL SOCIETY A MATHEMATICAL, PHYSICAL & ENGINEERING SCIENCES
PHILOSOPHICAL TRANSACTIONS OF THE ROYAL SOCIETY A MATHEMATICAL, PHYSICAL & ENGINEERING SCIENCES

Downloaded from rsta.royalsocietypublishing.org

Thus by performing a least squares fit of $\lg \alpha$ against $\lg f$ the power of the frequency dependence, s, could be obtained from the coefficient of the linear term. It was found that at 10 kPa

$$\lg \alpha_{\text{K.H.}} = \begin{Bmatrix} -4.09 \\ \pm 0.30 \end{Bmatrix} + \begin{Bmatrix} 0.498 \\ \pm 0.084 \end{Bmatrix} \lg f, \tag{44}$$

so that $s = 0.50 \pm 0.08$ (standard error), in agreement with the theoretical value of $\frac{1}{2}$. An estimate for the constant term based on such values of the transport properties of argon as were to hand (see table 3) gave, using equation (14),

$$\lg\left(\frac{A\pi^{\frac{1}{2}}}{bc_0}\right) = -4.12 \tag{45}$$

again, in good agreement with the measured value of -4.09 ± 0.30. Similar measurements made at 200 kPa gave the following results:

$$\lg \alpha_{\text{K.H.}} = \begin{Bmatrix} -4.63 \\ \pm 0.13 \end{Bmatrix} + \begin{Bmatrix} 0.460 \\ \pm 0.038 \end{Bmatrix} \lg f, \tag{46}$$

so that $s = 0.46 \pm 0.04$ (standard error) and the theoretical value of

$$\lg\left(\frac{A\pi^{\frac{1}{2}}}{bc_0}\right) = -4.77 \tag{47}$$

is in good agreement with the measured value of 4.63 ± 0.13. If the frequency dependence, $s = \frac{1}{2}$, is now assumed a better check on the value for A may be calculated by fitting α directly against $f^{\frac{1}{2}}$. Two least squares fits were made for each of the two pressures. The first fit was of the form $\alpha = a + bf^{\frac{1}{2}}$ and the second of the form $\alpha = bf^{\frac{1}{2}}$. At both the higher and the lower pressure the value of the constant term, a, differed from zero by less than two standard errors and so is not statistically significant. Indeed we should expect sound propagation to be a more reversible process at lower frequencies, i.e. that α extrapolated to zero frequency should vanish. For this reason we calculate A from the linear coefficient, b, of the second fit and find at 10 and 200 kPa

$$A = 2.07 \pm 0.06 \quad \text{(std error)}$$

and

$$A = 0.441 \pm 0.007 \text{ (std error)},$$

respectively, whereas we calculate from the values of table 3 the corresponding theoretical values

$$A = 1.98,$$

$$A = 0.44,$$

where A is expressed in units of cm $\text{s}^{-\frac{1}{2}}$. Again, agreement is satisfactory.

The effect of the boundary layer on measured velocity has also been investigated. We expect

$$c = c_\infty - \left(\frac{Ac_0}{2b\pi^{\frac{1}{2}}}\right) f^s \tag{48}$$

where $s = -\frac{1}{2}$. In order to check this a least squares fit of c against $f^{-\frac{1}{2}}$ was carried out to arrive at an estimate of c_∞ which is the measured velocity at infinite frequency. At the lower pressure it was found that

$$c = \begin{pmatrix} 307.46 \\ \pm 0.66 \end{pmatrix} - \begin{pmatrix} 94 \\ \pm 37 \end{pmatrix} f^{-\frac{1}{2}} \tag{49}$$

Downloaded from rsta.royalsocietypublishing.org

and at the higher pressure

$$c = \begin{pmatrix} 308.142 \\ \pm 0.058 \end{pmatrix} - \begin{pmatrix} 29.2 \\ \pm 3.2 \end{pmatrix} f^{-\frac{1}{2}}. \tag{50}$$

In order to check that the values of c_∞ thus obtained are consistent with the assumption that $\Delta c \propto f^{-\frac{1}{2}}$, the above values for c_∞ were subtracted from c to give Δc. Then $\lg (c - c_\infty)$ was fitted as a function of $\lg f$:

$$\lg (c - c_\infty) = \lg \left(\frac{A c_0}{2b\pi^{\frac{1}{2}}} \right) + s \lg f. \tag{51}$$

At the lower pressure we found

$$\lg (c_\infty - c) = \begin{pmatrix} 2.12 \\ \pm 0.66 \end{pmatrix} - \begin{pmatrix} 0.54 \\ \pm 0.19 \end{pmatrix} \lg f \tag{52}$$

giving $\Delta c \propto f^{-0.54 \pm 0.19}$ and at the higher pressure

$$\lg (c_\infty - c) = \begin{pmatrix} 1.57 \\ \pm 0.20 \end{pmatrix} - \begin{pmatrix} 0.536 \\ \pm 0.057 \end{pmatrix} \lg f \tag{53}$$

so that $\Delta c \propto f^{-0.54 \pm 0.06}$ thus showing our original assumption that $s = -\frac{1}{2}$ was consistent with the experimental results.

In addition we find that resulting values of A are consistent with the calculated ones. At 10 kPa we obtain from the constant term in the linear fit

$$A = 1.63 \pm 0.64 \text{ (standard error)}$$

which is compatible with the theoretical value of 1.98. At 200 kPa we find

$$A = 0.395 \pm 0.034 \text{ (standard error)}$$

which is just less than two standard errors from the theoretical value of 0.44. A better approach to checking the frequency dependence of Δc is to correct c in the recommended way and then to show that no frequency dependence remains in the corrected data. Fits of the form $c = a + bf^{-\frac{1}{2}}$ and $c = a + bf^{-\frac{1}{2}} + cf^{-1}$ were made at the two pressures and in all cases the coefficients of the f terms were less than the standard errors assigned to them. We conclude, therefore, that the performance of our instrument is compatible with the boundary layer theory.

But while these results are encouraging in that they rule out any unexpectedly large deviation from the orthodox boundary layer theory, they are not to be taken as having directly verified the theory to the accuracy to which we need to use it. Our results are still dependent on the minimum theoretical assumption of § 2.2 (equation (20)). However, it does seem most unlikely that the substantially correct frequency dependences and constants of proportionality for absorption coefficients and velocities would arise from a theory which was in error at such a fundamental level as this.

Agreement might have been somewhat better, but for a small effect observed at the two lower frequencies where it seems that higher harmonics of the fundamental frequency were excited. These can arise from some slight non-linearity of the diaphragm. In the case of the second harmonic, we would expect a small circle to be executed at the antiresonance of every fundamental circle and another – almost certainly unresolved – to be directly superimposed on the main circle itself. This was in fact observed at the 3 kHz points taken at 200 kPa where the harmonic circles at antiresonance had diameters of approximately 1.5 % of the main circles and correspondingly anomalous residuals seemed to be present in the fits to the absorption coefficient

Downloaded from rsta.royalsocietypublishing.org

data. No such effect was observed at 1.98 kHz at the same pressure where both second and third harmonic distortions were possible in principle. At the lower pressure of 10 kPa noise was generally too great at antiresonance to see such small irregularities. We emphasize that this effect cannot interfere with the results taken at 5.6 kHz from which the gas constant is calculated. As will be seen, no distortion was ever observed at antiresonance where generally the circles coincided exactly and regularly to better than the width of the line drawn by the pen (see figure 11). Further support is lent to the reliability of our boundary layer corrections by the excellent agreement found between calculated values of $\alpha_{\mathrm{K.H.}}$ (table 3) and those measured values used to make the final corrections (figure 16).

5. Results

Ninety-eight measurements of sound velocity and absorption coefficient were taken between 30 and 200 kPa (see figure 15 and table 4). Acoustic absorption coefficients were also measured down to 10 kPa to assist in making the necessary boundary layer corrections. But velocities at these lower pressures were difficult to measure with a useful accuracy. The following discussion of the way in which this data was processed is summarized in table 8 together with any associated uncertainties.

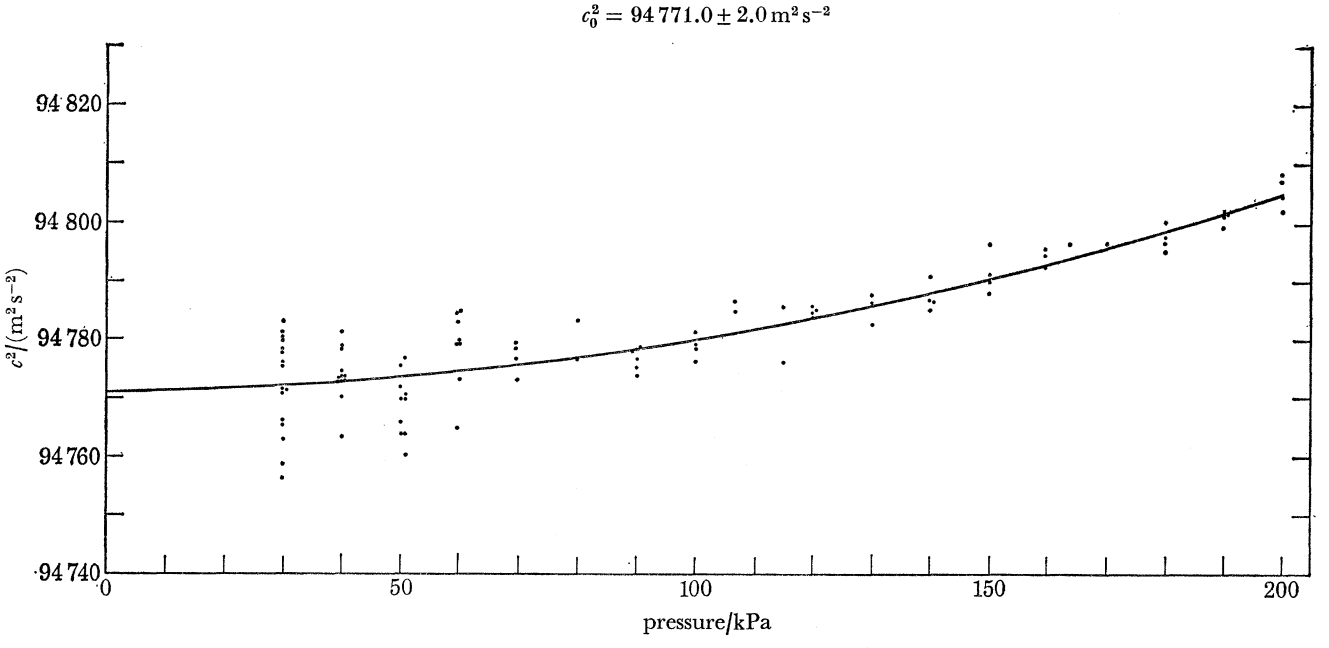

Figure 15. The acoustic isotherm at the triple point of water, showing the quadratic curve fitted to the data points (see table 6).

In order to take advantage of the theoretical expectation that the extrapolated absorption coefficient would be infinite at zero pressure, a least squares fit passing through the origin was made of $1/\alpha_{\mathrm{K.H.}}$ against the square root of the pressure (see figure 16 and table 5). Again, the measured absorption coefficient, α, was corrected for α_0 to give $\alpha_{\mathrm{K.H.}}$ from equation (41) and table 3 and it was increased by 1.71 % to account for the instrument correction discussed in § 4.2. Calculated values for α_0 over the pressure range 10–200 kPa range from 1.0 to 0.23% of $\alpha_{\mathrm{K.H.}}$ and so in making this small correction to α we felt justified in proceeding in the same way as for the

Downloaded from rsta.royalsocietypublishing.org

Table 4. Velocity and absorption coefficient data for the acoustic isotherm at 273 K

pressure/kPa	$c^2/(\mathrm{m^2\,s^{-2}})$ (measured)	$\alpha_{\mathrm{K.H.}}/\mathrm{m^{-1}}$ (measured)	$c^2/(\mathrm{m^2\,s^{-2}})$ (corrected using smoothed $\alpha_{\mathrm{K.H.}}$, etc)†
200 578	94 597.1	0.1248	94 804.7
200 589	94 594.5	0.1258	94 802.1
200 562	94 600.8	0.1252	94 808.4
200 507	94 599.5	0.1257	94 807.1
190 199	94 588.6	0.1293	94 801.7
190 164	94 588.9	0.1294	94 802.0
190 130	94 586.1	0.1296	94 799.3
190 095	94 588.1	0.1294	94 801.3
180 298	94 578.6	0.1324	94 797.5
180 298	94 576.4	0.1332	94 795.3
179 919	94 581.2	0.1310	94 800.4
179 850	94 578.0	0.1333	94 797.1
170 218	94 571.5	0.1353	94 796.7
163 564	94 566.8	0.1396	94 796.5
159 428	94 562.1	0.1408	94 794.7
159 462	94 560.0	0.1409	94 792.7
159 496	94 563.2	0.1417	94 795.8
150 147	94 556.9	0.1446	94 796.7
150 147	94 551.6	0.1469	94 791.3
150 182	94 550.5	0.1453	94 790.2
150 216	94 548.5	0.1451	94 788.2
140 060	94 538.5	0.1496	94 786.6
140 060	94 543.0	0.1490	94 791.1
140 046	94 538.7	0.1499	94 786.8
139 908	94 537.1	0.1493	94 785.3
130 035	94 529.0	0.1557	94 786.5
130 035	94 530.3	0.1545	94 787.8
130 035	94 525.3	0.1561	94 782.8
119 927	94 516.9	0.1613	94 784.9
119 927	94 516.1	0.1633	94 784.1
119 927	94 517.7	0.1633	94 785.8
119 927	94 516.8	0.1631	94 784.9
109 896	94 496.5	0.1692	94 776.4
109 896	94 505.9	0.1696	94 785.8
106 621	94 501.0	0.1712	94 785.1
106 655	94 502.6	0.1724	94 786.8
99 884	94 485.2	0.1778	94 778.7
99 884	94 485.8	0.1780	94 779.3
99 850	94 487.9	0.1766	94 781.5
99 850	94 482.9	0.1767	94 776.5
89 887	94 469.5	0.1860	94 778.9
89 887	94 469.2	0.1865	94 778.6
89 853	94 466.2	0.1883	94 775.6
89 853	94 469.4	0.1885	94 778.8
89 853	94 467.7	0.1876	94 777.0
89 853	94 464.6	0.1883	94 774.0
79 745	94 448.8	0.2003	94 777.0
79 745	94 455.1	0.1999	94 783.4
69 472	94 428.3	0.2114	94 779.8
69 472	94 427.2	0.2165	94 778.7
69 472	94 425.4	0.2126	94 776.9
69 437	94 422.0	0.2115	94 773.6
59 750	94 401.2	0.2312	94 780.0
59 722	94 394.7	0.2326	94 773.6

† All the corrections made in the text (see table 8) have been carried out to obtain this value.

PHILOSOPHICAL TRANSACTIONS OF THE ROYAL SOCIETY A MATHEMATICAL, PHYSICAL & ENGINEERING SCIENCES

PHILOSOPHICAL TRANSACTIONS OF THE ROYAL SOCIETY A MATHEMATICAL, PHYSICAL & ENGINEERING SCIENCES

Downloaded from rsta.royalsocietypublishing.org

TABLE 4 (*cont.*)

pressure/kPa	$c^2/(\mathrm{m^2\,s^{-2}})$ (measured)	$\alpha_{\mathrm{R.H.}}/\mathrm{m^{-1}}$ (measured)	$c^2/(\mathrm{m^2\,s^{-2}})$ (corrected using smooth $\alpha_{\mathrm{K.H.}}$, etc.)
59 702	94 406.4	0.2305	94 785.4
59 702	94 401.5	0.2288	94 780.5
59 681	94 406.2	0.2304	94 785.3
59 633	94 404.0	0.2297	94 783.2
59 564	94 385.9	0.2283	94 765.3
59 543	94 400.1	0.2322	94 779.6
50 718	94 349.8	0.2517	94 760.6
50 711	94 359.2	0.2514	94 770.1
50 711	94 360.0	0.2505	94 770.9
50 711	94 366.6	0.2495	94 777.5
50 697	94 359.5	0.2494	94 770.4
50 649	94 353.0	0.2495	94 764.0
49 835	94 361.4	0.2528	94 775.9
49 835	94 351.9	0.2562	94 766.3
49 822	94 349.9	0.2508	94 764.4
49 822	94 358.0	0.2551	94 772.5
40 114	94 312.0	0.2832	94 773.5
40 114	94 309.4	0.2816	94 770.9
40 203	94 313.3	0.2814	94 774.3
40 203	94 320.9	0.2798	94 782.0
40 196	94 314.2	0.2849	94 775.2
40 196	94 318.6	0.2792	94 779.7
40 148	94 312.0	0.2824	94 773.4
40 148	94 312.2	0.2820	94 773.5
40 148	94 312.1	0.2812	94 773.4
40 148	94 317.6	0.2806	94 779.0
40 107	94 312.8	0.2826	94 774.4
40 100	94 302.4	0.2842	94 763.9
29 965	94 243.8	0.3265	94 777.0
29 965	94 248.2	0.3233	94 781.5
29 965	94 247.4	0.3253	94 780.6
29 965	94 248.9	0.3269	94 782.1
29 965	94 233.7	0.3246	94 766.8
29 965	94 224.4	0.3279	94 757.4
29 958	94 226.7	0.3304	94 759.8
29 958	94 239.0	0.3282	94 772.2
29 958	94 245.5	0.3282	94 778.8
29 944	94 250.5	0.3239	94 784.0
29 944	94 245.2	0.3333	94 778.7
29 944	94 233.1	0.3335	94 766.4
29 944	94 243.1	0.3260	94 776.5
29 944	94 230.4	0.3278	94 763.7
29 916	94 239.3	0.3282	94 772.9
29 916	94 239.5	0.3277	94 773.1
19 891		0.3994	
19 891		0.3840	
19 891		0.4077	
10 101		0.5618	
10 101		0.5544	
10 101		0.5582	
10 101		0.5611	

PHILOSOPHICAL TRANSACTIONS OF THE ROYAL SOCIETY A MATHEMATICAL, PHYSICAL & ENGINEERING SCIENCES

PHILOSOPHICAL TRANSACTIONS OF THE ROYAL SOCIETY A MATHEMATICAL, PHYSICAL & ENGINEERING SCIENCES

Downloaded from rsta.royalsocietypublishing.org

boundary layer investigations. At n.t.p. α_0 is 0.3 % of $\alpha_{\mathrm{K.H.}}$ and the boundary layer correction represents a change of about 1.5×10^{-3} in the velocity so that if α_0 is in error by as much as 10 % it only affects the calculated velocity by 0.5 p.p.m. which, in our case, is insignificant. Strictly speaking $\alpha_{\mathrm{K.H.}}^{-1}$ is proportional to $\rho^{\frac{1}{2}}$ rather than $p^{\frac{1}{2}}$ (see equation (41)) but at these pressures and this temperature the error due to taking $p^{\frac{1}{2}}$ is negligible. This fit enabled us to calculate a smoothed boundary layer correction for each isotherm point. The statistical uncertainty at a given pressure in the boundary layer correction arising from the statistical uncertainty in the smoothed absorption coefficients is equal to the fractional standard error in the coefficient of the $1/\alpha_{\mathrm{K.H.}}$ against $p^{\frac{1}{2}}$ fit multiplied by c^2/ω (see equation (13)). To obtain the uncertainty in the intercept of the isotherm arising from this statistical uncertainty in the boundary layer correction, the latter has to be extrapolated to zero pressure. We then combine it in quadrature with the statistical uncertainty in the intercept arising from the isotherm least squares fit.

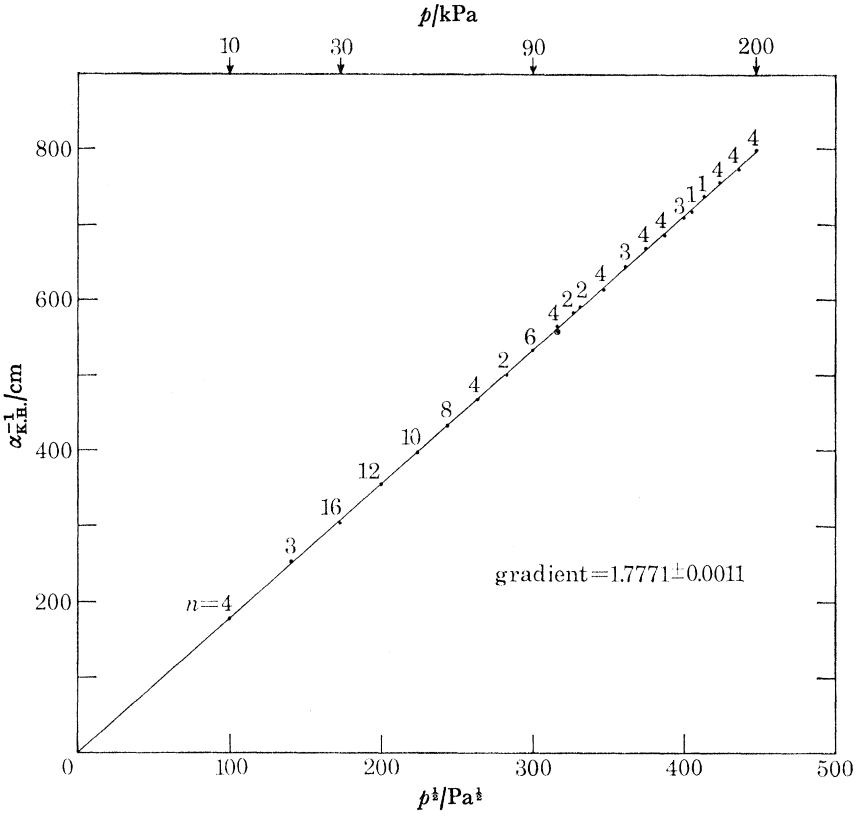

FIGURE 16. The reciprocal boundary layer absorption coefficient plotted against the square root of the pressure. ●, Average of measured points; n, number of measurements of $\alpha_{\mathrm{K.H.}}$ at each pressure; ⊙, theoretical point calculated from table 3.

The boundary layer correction to the measured velocity was the greatest single adjustment to be made, being at the 1000 p.p.m. level. But five other corrections were also made at the 10 p.p.m. level and below. Firstly, all velocities were corrected for temperature drift during a measurement and for small errors in the realization of the triple point of water (§ 4.1). These corrections might amount to 30 p.p.m., but were usually far less. Their accuracy depends uopn the uncertainty in the calibration of the platinum resistance thermometer, which was less than 0.3 mK (equivalent

Downloaded from rsta.royalsocietypublishing.org

TABLE 5. LINEAR FIT OF RECIPROCAL BOUNDARY LAYER ABSORPTION COEFFICIENTS AGAINST THE SQUARE ROOT OF THE PRESSURE AT 273 K

$10^{-2}(\alpha_{\mathrm{K.H.}}/\mathrm{cm}^{-1})^{-1}$ $(10^{-2}Y(\mathrm{data}))$	$10^{-2}p^{\frac{1}{2}}/\mathrm{Pa}^{\frac{1}{2}}$ $(10^{-2}X(\mathrm{data}))$	$10^{-2}(\alpha_{\mathrm{K.H.}}/\mathrm{cm}^{-1})^{-1}$ $(10^{-2}Y(\mathrm{calc.}))$	residuals
8.012 10	4.478 59	7.958 93	+5.3
7.947 33	4.478 72	7.959 15	−1.2
7.986 07	4.478 41	7.958 61	+2.7
7.953 77	4.477 80	7.957 52	−0.4
7.737 51	4.361 18	7.750 27	−1.5
7.729 64	4.360 78	7.748 56	−2.0
7.717 50	4.360 39	7.748 87	−3.1
7.729 64	4.359 99	7.748 16	−1.9
7.552 49	4.246 15	7.545 85	+0.7
7.506 36	4.246 15	7.545 85	−3.9
7.634 64	4.241 69	7.537 92	+9.7
7.500 68	4.240 87	7.536 47	−3.6
7.388 96	4.125 75	7.331 89	+5.7
7.163 59	4.044 30	7.187 15	−2.4
7.101 97	3.992 84	7.095 70	+0.6
7.096 84	3.993 27	7.096 46	+0.0
7.056 09	3.993 70	7.097 21	−4.1
6.913 32	3.874 88	6.886 07	+2.7
6.808 00	3.874 88	6.886 07	−7.8
6.884 27	3.875 33	6.886 87	−0.3
6.893 92	3.875 77	6.887 65	+0.6
6.684 31	3.742 46	6.650 74	+3.4
6.711 69	3.742 46	6.650 74	+6.1
6.670 71	3.742 27	6.650 41	+2.0
6.697 99	3.740 43	6.647 13	+5.1
6.423 67	3.606 04	6.408 30	+1.5
6.474 43	3.606 04	6.408 30	+6.6
6.406 92	3.606 04	6.408 30	−0.1
6.198 39	3.463 05	6.154 20	+4.4
6.125 03	3.463 05	6.154 20	−2.9
6.125 03	3.463 05	6.154 20	−2.9
6.132 67	3.463 05	6.154 20	−2.2
5.909 43	3.315 06	5.891 20	+1.8
5.895 26	3.315 06	5.891 20	+0.4
5.839 80	3.265 29	5.802 76	+3.7
5.801 89	3.265 81	5.803 68	−0.2
5.623 89	3.160 44	5.616 44	+0.7
5.617 46	3.160 44	5.616 44	+0.1
5.662 77	3.159 91	5.615 48	+4.7
5.659 51	3.159 91	5.615 48	+4.4
5.376 74	2.998 12	5.327 97	+4.9
5.362 08	2.998 12	5.327 97	+3.4
5.309 96	2.99755	5.326 96	−1.7
5.304 23	2.997 55	5.326 96	−2.3
5.330 11	2.997 55	5.326 96	+0.3
5.309 96	2.997 55	5.326 96	−1.7
4.991 36	2.823 92	5.018 39	−2.7
5.001 52	2.823 92	5.018 39	−1.7
4.729 80	2.635 75	4.684 01	+4.6
4.618 70	2.635 75	4.684 01	−6.5
4.702 65	2.635 75	4.684 01	+1.9
4.727 53	2.635 09	4.682 83	+4.5
4.324 82	2.444 38	4.343 92	−1.9
4.298 36	2.443 81	4.342 90	−4.5
4.338 19	2.443 40	4.342 18	−0.4
4.370 98	2.443 40	4.342 18	+2.9

PHILOSOPHICAL TRANSACTIONS OF THE ROYAL SOCIETY A MATHEMATICAL, PHYSICAL & ENGINEERING SCIENCES

PHILOSOPHICAL TRANSACTIONS OF THE ROYAL SOCIETY A MATHEMATICAL, PHYSICAL & ENGINEERING SCIENCES

Downloaded from rsta.royalsocietypublishing.org

TABLE 5 (*cont.*)

$10^{-2}(\alpha_{\mathrm{K.H.}}/\mathrm{cm}^{-1})^{-1}$ $(10^{-2}Y(\mathrm{data}))$	$10^{-2}p^{\frac{1}{2}}/\mathrm{Pa}^{\frac{1}{2}}$ $(10^{-2}X(\mathrm{data}))$	$10^{-2}(\alpha_{\mathrm{K.H.}}/\mathrm{cm}^{-1})^{-1}$ $10^{-2}\,Y$ (calc.)	residuals
4.340 11	2.442 97	4.341 41	−0.1
4.353 58	2.441 99	4.339 67	+1.4
4.380 76	2.440 57	4.337 15	+4.4
4.305 94	2.440 14	4.336 39	−3.0
3.973 05	2.252 07	4.002 16	−2.9
3.977 87	2.251 91	4.001 88	−2.4
3.992 41	2.251 91	4.001 88	−0.9
4.008 69	2.251 91	4.001 88	+0.7
4.010 33	2.251 60	4.001 33	+0.9
4.008 71	2.250 53	3.999 43	+0.9
3.955 78	2.232 38	3.967 16	−1.1
3.903 95	2.232 38	3.967 16	−6.3
3.987 88	2.232 08	3.966 65	+2.1
3.919 52	2.232 08	3.966 65	−4.7
3.530 75	2.002 85	3.559 27	−2.9
3.551 15	2.002 85	3.559 27	−0.8
3.553 68	2.005 07	3.563 22	−1.0
3.574 35	2.005 07	3.563 22	+1.1
3.510 54	2.004 89	3.562 91	−5.2
3.582 17	2.004 89	3.562 91	+1.9
3.540 91	2.003 70	3.560 78	−2.0
3.546 02	2.003 70	3.560 78	−1.5
3.556 28	2.003 70	3.560 78	−0.5
3.564 01	2.003 70	3.560 78	+0.3
3.538 38	2.002 67	3.558 96	−2.1
3.518 12	2.002 50	3.558 65	−4.1
3.063 10	1.731 04	3.076 24	−1.3
3.092 97	1.731 04	3.076 24	+1.7
3.073 63	1.731 04	3.076 24	−0.3
3.059 29	1.731 04	3.076 24	−1.7
3.080 37	1.731 04	3.076 24	+0.4
3.049 80	1.731 04	3.076 24	−2.6
3.026 33	1.730 84	3.075 88	−5.0
3.046 97	1.730 84	3.075 88	−2.9
3.046 97	1.730 84	3.075 88	−2.9
3.087 16	1.730 43	3.075 16	+1.2
3.000 48	1.730 43	3.075 16	−7.5
2.998 65	1.730 43	3.075 16	−7.7
3.067 89	1.730 43	3.075 16	−0.7
3.050 76	1.730 43	3.075 16	−2.4
3.046 99	1.729 62	3.073 72	−2.7
3.051 72	1.729 62	3.073 72	−2.2
2.503 63	1.410 35	2.506 35	−0.3
2.604 44	1.410 35	2.506 35	+9.8
2.453 04	1.410 35	2.506 35	−5.3
1.779 85	1.005 04	1.786 06	−0.6
1.803 69	1.005 04	1.786 06	+1.8
1.791 53	1.005 04	1.786 06	+0.5
1.782 11	1.005 04	1.786 06	−0.4

Result: $1/\alpha_{\mathrm{K.H.}} = \begin{pmatrix} 1.77710 \\ \pm 0.00114 \end{pmatrix} p^{\frac{1}{2}}\,\mathrm{cm}$

r.m.s. deviation of $Y = 3.39\,\mathrm{cm}$

standard error of fit $= 3.41\,\mathrm{cm}$

PHILOSOPHICAL TRANSACTIONS OF THE ROYAL SOCIETY A MATHEMATICAL, PHYSICAL & ENGINEERING SCIENCES

PHILOSOPHICAL TRANSACTIONS OF THE ROYAL SOCIETY A MATHEMATICAL, PHYSICAL & ENGINEERING SCIENCES

Downloaded from rsta.royalsocietypublishing.org

to 1 p.p.m. in R), and on any possible temperature difference between the thermometer and the argon in the cavity. We put an upper limit of 1 mK on the latter which is large compared to the observed temperature change in the interferometer (see figure 10). Thus an overall systematic uncertainty of 5 p.p.m. arises in the value of the gas constant from this source. The second order correction of Shields *et al.* to the boundary layer theory of Kirchhoff and Helmholtz was equivalent to approximately -25 p.p.m. at the lowest isotherm pressures (§ 2.2) where the allowance for the refractive index of argon (which extrapolates to zero with the isotherm extrapolation in any case) is 84 p.p.m. (§ 3.1). Compensation for the approximations in the first order theory of the interferometer (appendix B) amounted to about 7 p.p.m. at 30 kPa. A further correction has been made for molecular slip according to the equation

$$\frac{\Delta c}{c} = (\pi/2\gamma)^{\frac{1}{2}} c\eta \left(\frac{2-g}{g}\right) \Big/ b\left\{p + \left(\frac{2-g}{g}\right)(\pi\omega p\eta)^{\frac{1}{2}}\right\}, \tag{54}$$

where g is the fraction of molecules diffusely reflected from the cavity boundary at $r = b$. It can be seen that this relation, which arises as a small modification to the Kirchhoff–Helmholtz theory (Henry 1931; Weston 1953), predicts a finite effect even when $g = 1$. Following Shields *et al.* (1965) who under very similar circumstances found g to be unity in brass and steel tubes, we obtain corrections which, when extrapolated to zero pressure, amount to 40 p.p.m. to be subtracted from the isotherm intercept value. To allow for the possibility of g being as low as 0.9 we associate a 20 % uncertainty with this correction or 8 p.p.m. in the gas constant. A considerable body of experimental evidence from molecular beam studies now exists indicating that $g > 0.95$ for argon on smooth metal surfaces at room temperature (see, for example, Stickney & Hurlbut 1963).

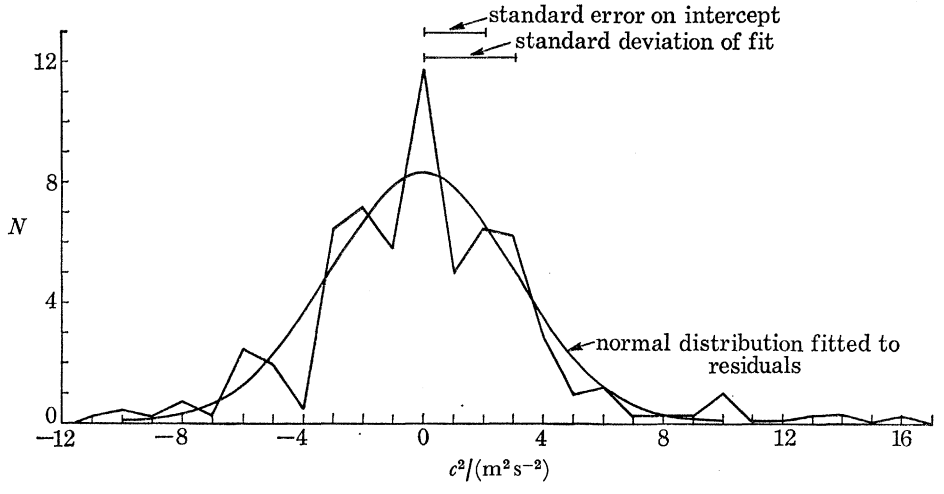

FIGURE 17. A histogram of the residuals of the least-squares quadratic fit of c^2 plotted against p shown in figure 15. N is the number of residuals $\times w^2$. For this histogram the residuals were taken from table 6 and rounded to the nearest integral $m^2 s^{-2}$.

Having made the necessary corrections the problem remains on how the isotherm is to be fitted. In principle an infinite polynomial of pressure terms is required, but the assumption is always made that the higher terms are negligible. Because of their increased scatter points below 65 kPa were given weighting $w^2 = 0.25$. We then fitted the data with several polynomials of increasing order until no improvement in the fit was found upon raising the order. In fact a quadratic

Downloaded from rsta.royalsocietypublishing.org

TABLE 6. LEAST SQUARES FITS TO ACOUSTIC ISOTHERM DATA

data points taken at pressures lower than 65 kPa have weights $w^2 = 0.25$
quadratic fit
r.m.s. deviation of $Y = 3.05\,\mathrm{m^2\,s^{-2}}$
standard deviation of fit $= 3.10\,\mathrm{m^2\,s^{-2}}$

term	coefficient	standard error
0	$9.477\,10 \times 10^{+4}$	$1.954\,97 \times 10^{+0}$
1	$1.622\,89 \times 10^{-5}$	$3.691\,20 \times 10^{-5}$
2	$7.604\,11 \times 10^{-10}$	$1.550\,89 \times 10^{-10}$

$10^{-4}p$/Pa ($10^{-4}X$(data))	$10^{-4}c^2/(\mathrm{m^2\,s^{-2}})$ (corrected for boundary layer, etc.) ($10^{-4}Y$(data))	$10^{-4}c^2/(\mathrm{m^2\,s^{-2}})$ ($10^{-4}Y$(calc.))	residuals
2.9916	9.477 21	9.477 22	+ 0.1
2.9916	9.477 19	9.477 22	+ 0.3
2.9944	9.476 27	9.477 22	+ 9.5
2.9944	9.477 54	9.477 22	− 3.3
2.9944	9.476 54	9.477 22	+ 6.8
2.9944	9.477 76	9.477 22	− 5.5
2.9944	9.478 30	9.477 22	−10.8
2.9958	9.477 78	9.477 22	− 5.6
2.9958	9.477 12	9.477 22	+ 1.0
2.9958	9.475 88	9.477 22	+13.4
2.9965	9.475 64	9.477 22	+15.8
2.9965	9.476 58	9.477 22	+ 6.4
2.9965	9.478 11	9.477 22	− 8.9
2.9965	9.477 96	9.477 22	− 7.4
2.9965	9.478 04	9.477 22	− 8.2
2.9965	9.477 60	9.477 22	− 3.8
4.0100	9.476 31	9.477 29	+ 9.8
4.0107	9.477 36	9.477 29	− 0.7
4.0148	9.477 82	9.477 29	− 5.3
4.0148	9.477 27	9.477 29	+ 0.2
4.1048	9.477 28	9.477 29	+ 0.1
4.0148	9.477 26	9.477 29	+ 0.3
4.0196	9.477 89	9.477 29	− 6.0
4.0196	9.477 45	9.477 29	− 1.6
4.0203	9.478 12	9.477 29	− 8.3
4.0203	9.477 35	9.477 29	− 0.6
4.0114	9.477 01	9.477 29	+ 2.8
4.0114	9.477 27	9.477 29	+ 0.2
4.9835	9.477 18	9.477 37	+ 1.9
4.9835	9.476 37	9.477 37	+10.0
4.9822	9.476 57	9.477 37	+ 8.0
4.9822	9.477 53	9.477 37	− 1.6
5.0649	9.476 34	9.477 38	+10.4
5.0697	9.477 98	9.477 38	+ 4.0
5.0711	9.477 69	9.477 38	− 3.1
5.0711	9.477 03	9.477 38	+ 3.5
5.0711	9.477 95	9.477 38	+ 4.3
5.0718	9.476 00	9.477 38	+13.8
5.9543	9.477 91	9.477 47	− 4.4
5.9564	9.476 48	9.477 47	+ 9.9
5.9633	9.478 27	9.477 47	− 8.0
5.9681	9.478 48	9.477 47	−10.1
5.9750	9.477 99	9.477 47	− 5.2
5.9722	9.478 49	9.477 47	−10.2
5.9702	9.477 31	9.477 47	+ 1.6

PHILOSOPHICAL TRANSACTIONS OF THE ROYAL SOCIETY A MATHEMATICAL, PHYSICAL & ENGINEERING SCIENCES
PHILOSOPHICAL TRANSACTIONS OF THE ROYAL SOCIETY A MATHEMATICAL, PHYSICAL & ENGINEERING SCIENCES

Downloaded from rsta.royalsocietypublishing.org

TABLE 6 (*cont.*)

$10^{-4}p$/Pa ($10^{-4}X$(data))	$10^{-4}c^2/(\mathrm{m^2\,s^{-2}})$ (corrected for boundary layer, etc.) ($10^{-4}Y$(data))	$10^{-4}c^2/(\mathrm{m^2\,s^{-2}})$ ($10^{-4}Y$(calc.))	residuals
5.9702	9.477 97	9.477 47	− 5.0
6.9437	9.477 31	9.477 58	+ 2.7
6.9472	9.477 65	9.477 58	− 0.6
6.9472	9.477 83	9.477 58	− 2.4
6.9472	9.477 94	9.477 58	− 3.5
7.9745	9.478 30	9.477 71	− 5.9
7.9745	9.477 66	9.477 71	+ 0.5
8.9853	9.477 36	9.477 86	+ 5.0
8.9853	9.477 67	9.477 86	+ 1.9
8.9853	9.477 84	9.477 86	+ 0.2
8.9853	9.477 52	9.477 86	+ 3.4
8.9887	9.477 82	9.477 86	+ 0.4
8.9887	9.477 85	9.477 86	+ 0.1
9.9850	9.477 62	9.478 02	+ 4.1
9.9850	9.478 12	9.478 02	− 0.9
9.9884	9.477 90	9.478 02	+ 1.2
9.9884	9.477 84	9.478 02	+ 1.9
10.6655	9.478 65	9.478 14	− 5.1
10.6621	9.478 49	9.478 14	− 3.5
10.9896	9.478 55	9.478 20	− 3.5
10.9896	9.477 61	9.478 20	+ 5.9
11.9927	9.478 46	9.478 39	− 0.7
11.9927	9.478 55	9.478 39	− 1.6
11.9927	9.478 39	9.478 39	+ 0.0
11.9927	9.478 47	9.478 39	− 0.8
13.0035	9.478 26	9.478 60	+ 3.4
13.0035	9.478 76	9.478 60	− 1.6
13.0035	9.478 62	9.478 60	− 0.3
13.9908	9.478 51	9.478 82	+ 3.0
14.0046	9.478 66	9.478 82	+ 1.6
14.0060	9.479 09	9.478 82	− 2.7
14.0060	9.478 64	9.478 82	+ 1.8
15.0216	9.478 80	9.479 06	+ 2.7
15.0182	9.479 00	9.479 06	+ 0.6
15.0147	9.479 11	9.479 06	− 0.5
15.0147	9.479 64	9.479 06	− 5.9
15.9496	9.479 56	9.479 29	− 2.7
15.9462	9.479 25	9.479 29	+ 0.5
15.9428	9.479 45	9.479 29	− 1.6
16.3564	9.479 64	9.479 40	− 2.3
17.0218	9.479 65	9.479 58	− 0.7
17.9850	9.479 69	9.4798 5	+ 1.6
17.9919	9.480 02	9.479 86	− 1.6
18.0298	9.479 51	9.479 87	+ 3.6
18.0298	9.479 73	9.479 87	+ 1.3
19.0095	9.480 11	9.480 16	+ 0.5
19.0130	9.479 91	9.480 16	+ 2.4
19.0164	9.480 19	9.480 16	− 0.3
19.0199	9.480 15	9.480 16	+ 0.1
20.0507	9.480 70	9.480 48	− 2.1
20.0562	9.480 82	9.480 49	− 3.4
20.0589	9.480 20	9.480 49	+ 2.9
20.0578	9.480 45	9.480 49	+ 0.3

PHILOSOPHICAL TRANSACTIONS OF THE ROYAL SOCIETY A MATHEMATICAL, PHYSICAL & ENGINEERING SCIENCES

PHILOSOPHICAL TRANSACTIONS OF THE ROYAL SOCIETY A MATHEMATICAL, PHYSICAL & ENGINEERING SCIENCES

Downloaded from rsta.royalsocietypublishing.org

TABLE 6 (*cont.*)

result of quadratic fit (above)

$$c^2 = \begin{pmatrix} 94\,771.0 \\ \pm 2.0 \end{pmatrix} + \begin{pmatrix} 1.6 \\ \pm 3.7 \end{pmatrix} \times 10^{-5} p + \begin{pmatrix} 7.60 \\ \pm 1.55 \end{pmatrix} \times 10^{-10} p^2$$

result of linear fit (not shown)

r.m.s. deviation of $Y = 3.49\,\mathrm{m^2\,s^{-2}}$

standard deviation of fit $= 3.52\,\mathrm{m^2\,s^{-2}}$

$$c^2 = \begin{pmatrix} 94\,760.2 \\ \pm 1.1 \end{pmatrix} + \begin{pmatrix} 2.100 \\ \pm 0.086 \end{pmatrix} \times 10^{-4} p$$

result of cubic fit (not shown)

r.m.s. deviation of $Y = 3.05\,\mathrm{m^2\,s^{-2}}$

standard deviation of fit $= 3.12\,\mathrm{m^2\,s^{-2}}$

$$c^2 = 94\,771.9 - (1.3 \times 10^{-5})\,p + (10.27 \times 10^{-10})\,p^2 - (7.4 \times 10^{-16})\,p^3$$

TABLE 7. LEAST SQUARES FITS TO TRUNCATED ISOTHERM DATA

number of points fitted	linear fit: $c^2 = a + bp$	quadratic fit: $c^2 = a + bp + cp^2$
98	$a = 94\,760.2 \pm 1.1\,\mathrm{m^2\,s^{-2}}$ $b = (2.10 \pm 0.09) \times 10^{-4}\,\mathrm{m^2\,s^{-2}\,Pa^{-1}}$ standard deviation of fit $= 3.52$	$a = 94\,771.0 \pm 2.0\,\mathrm{m^2\,s^{-2}}$ $b = (1.6 \pm 3.7) \times 10^{-5}\,\mathrm{m^2\,s^{-2}\,Pa^{-1}}$ $c = (7.60 \pm 1.55) \times 10^{-10}\,\mathrm{m^2\,s^{-2}\,Pa^{-2}}$ standard deviation of fit $= 3.10$
74	$a = 94\,766.2 \pm 1.5\,\mathrm{m^2\,s^{-2}}$ $b = (1.43 \pm 0.17) \times 10^{-4}\,\mathrm{m^2\,s^{-2}\,Pa^{-1}}$ standard deviation of fit $= 3.34$	$a = 94\,770.5 \pm 3.3\,\mathrm{m^2\,s^{-2}}$ $b = (3.78 \pm 8.95) \times 10^{-5}\,\mathrm{m^2\,s^{-2}\,Pa^{-1}}$ $c = (5.93 \pm 5.46) \times 10^{-10}\,\mathrm{m^2\,s^{-2}\,Pa^{-2}}$ standard deviation of fit $= 3.33$
50	$a = 94\,767.4 \pm 3.0\,\mathrm{m^2\,s^{-2}}$ $b = (13.38 \pm 0.58) \times 10^{-5}\,\mathrm{m^2\,s^{-2}\,Pa^{-1}}$ standard deviation of fit $= 3.48$	$a = 94\,779.9 \pm 12.3\,\mathrm{m^2\,s^{-2}}$ $b = (4.1 \pm 5.3) \times 10^{-4}\,\mathrm{m^2\,s^{-2}\,Pa^{-1}}$ $c = (5.2 \pm 5.3) \times 10^{-9}\,\mathrm{m^2\,s^{-2}\,Pa^{-2}}$ standard deviation of fit $= 3.47$
28	$a = 94767.8 \pm 9.0\,\mathrm{m^2\,s^{-2}}$ $b = (1.5 \pm 2.6) \times 10^{-4}\,\mathrm{m^2\,s^{-2}\,Pa^{-1}}$ standard deviation of fit $= 3.46$	$a = 102\,358 \pm 5569\,\mathrm{m^2\,s^{-2}}$ $b = -(4.4 \pm 3.2) \times 10^{-1}\,\mathrm{m^2\,s^{-2}\,Pa^{-1}}$ $c = (6.3 \pm 4.6) \times 10^{-6}\,\mathrm{m^2\,s^{-2}\,Pa^{-2}}$ standard deviation of fit $= 3.41$

polynomial was perfectly adequate (see figure 17 and table 6), the standard error in the intercept being 21 p.p.m. of c_0^2. The data was increasingly truncated to see if removing the higher pressure points produced data which was able to be represented by a linear fit with a consistent value for the intercept (see table 7). This was found to be the case, although the scatter in the 28 low pressure points was so large, and the distance of extrapolation so comparable with the range of data, that the standard error in the intercept became large enough to embrace nearly five standard errors on the original quadratic fit to all 98 points.

Since no improvement to the fit was found in raising the order of fit to three, it was decided to take the quadratic polynomial as the best fit to the data. In any case the intercept of the cubic fit differed from that of the quadratic by less than half the standard error on the intercept of the quadratic fit. The fractional standard error in the gradient of the $\alpha_{\mathrm{K.H.}}^{-1}$ against $p^{\frac{1}{2}}$ fit was 6.4×10^{-4} which represents the fractional error in the boundary layer corrections to c. This becomes 12.8×10^{-4} in the boundary layer correction to c^2. Extrapolating this error to zero pressure we find that it becomes 4.2 p.p.m. in c_0^2 which, when combined in quadrature with the standard error of 21 p.p.m. in the quadratic fit leads to a final unchanged statistical uncertainty (at the 67 % confidence level) of 21 p.p.m. Thus the final value for the intercept is

$$c_0^2 = 94\,771.0 \pm 2.0\,\mathrm{m^2/s^2},$$

Downloaded from rsta.royalsocietypublishing.org

TABLE 8. THE PROCEDURE FOR CALCULATING THE VALUE OF THE GAS CONSTANT AND CORRECTING FOR SYSTEMATIC EFFECTS IN THE MEASUREMENTS

measured quantity	correction to or source of intrinsic uncertainty in measured quantity	uncertainty in correction or intrinsic uncertainty in measured quantity	resulting uncertainty in c_0^2 and R	
			systematic	random
absorption coefficient	calculate and subtract classical absorption α_0, to give boundary layer absorption, $\alpha_{K.H.}$ $\alpha_{K.H.} = \alpha - \alpha_0$; $\alpha_0/\alpha = 0.25\,\% - 1\,\%$	$< 10\,\%\ \alpha_0$	< 0.5 p.p.m.	—
	instrument correction $1.71\,\%\ \alpha$	$0.18\,\%\ \alpha$	12 p.p.m.	—
	fit $\alpha_{K.H.}^{-1}$ against $p^{\frac{1}{2}}$ and calculate smoothed boundary layer correction $\Delta c/c = \alpha_{K.H.}/k$, $k = 2\pi/\lambda$ standard error in $\alpha_{K.H.} = 0.064\,\%$ at all pressures			
velocity, c	correct for temperature drift during measurement (typically 1 mK) and for error in triple point realization (typically 7 mK)	1.3 mK	5 p.p.m.	—
	correct for boundary layer using $\alpha_{K.H.}^{-1}$ fit; $\Delta c/c = 1.1 \times 10^{-3}$ at 200 kPa and 2.7×10^{-3} at 30 kPa	$0.064\,\%\ \Delta c$	—	4 p.p.m.*
	correct boundary layer theory $\Delta c/c = 3.4\ (\Delta c/c)^2$	$0.34\ (\Delta c/c)^2$	3 p.p.m.	—
	uncertainty in optical measurement of piston displacement	1.5 p.p.m.	3 p.p.m.	—
	raise value to allow for error in first order theory of interferometer. $\Delta c/c = (\alpha/k)^2$ $\Delta c_0/c_0 = 10$ p.p.m.	—	—	—
	decrease value to allow for effect of molecular slip $\Delta c_0/c_0 = 20$ p.p.m.	20 %	8 p.p.m.	—
	fit acoustic isotherm with quadratic: $c^2 = c_0^2 + A_1 p + A_2 p^2$ (95 d.f.) $c_0^2 = (94\,771.0 \pm 2.0)\ \mathrm{m^2\,s^{-2}}$ (4 p.p.m. error * above included). $A_1 = (1.62 \pm 3.69) \times 10^{-5}\ \mathrm{m^2\,s^{-2}\,Pa^{-1}}$ $A_2 = (7.60 \pm 1.55) \times 10^{-10}\ \mathrm{m^2\,s^{-2}\,Pa^{-2}}$ (standard errors quoted)			
molecular mass, M	uncertainty due to uncertainty in isotropic constitution and atomic masses of individual isotopes (2×10^{-4} g/mol)	5 p.p.m.	5 p.p.m.	—
	impurities < 10 p.p.m. nitrogen	4 p.p.m.	4 p.p.m.	—
	Result: $R = 8315.73 \pm 0.17\ \mathrm{J\,K^{-1}\,kmol^{-1}}$ (standard statistical error quoted) If systematic uncertainties are combined in quadrature an overall systematic uncertainty of 17 p.p.m. results.			

where the quoted uncertainty is one statistical standard error in a fit of 95 degrees of freedom. We may therefore calculate the gas constant from

$$c_0^2 = \gamma R T_0 / M,$$

where $\gamma = \frac{5}{3}$, $T_0 = 273.16\,\mathrm{K}$, $M = 39.9476\,\mathrm{g/mol}$, from which

$$R = \mathbf{8315.73 \pm 0.17\ J\,K^{-1}\,kmol^{-1}}.\dagger$$

† This value supersedes that published in our preliminary report (Quinn *et al.* 1974) which was lower by 17 p.p.m.

PHILOSOPHICAL TRANSACTIONS OF THE ROYAL SOCIETY A MATHEMATICAL, PHYSICAL & ENGINEERING SCIENCES

PHILOSOPHICAL TRANSACTIONS OF THE ROYAL SOCIETY A MATHEMATICAL, PHYSICAL & ENGINEERING SCIENCES

Downloaded from rsta.royalsocietypublishing.org

In addition to the errors discussed above (see table 8) it is also necessary to take account of the uncertainty of 5 p.p.m. in the molecular mass of the argon resulting from lack of knowledge of the isotopic composition of natural argon (§ 3.2). This leads directly to a possible systematic error of 5 p.p.m. in our value of the gas constant. The uncertainty in c due to impurities was mentioned in § 3.2 and shown to be equivalent to 2 p.p.m., or 4 p.p.m. in M and therefore R. No significant uncertainty in the gas constant arises from uncertainty in pressure or frequency.

We have attempted to justify the basic acoustic relations used in this work either by experimental tests or by theoretical argument and where it has been possible by both. The dependence of the boundary layer absorption coefficient and velocity correction upon the square root of the frequency is an example of the latter. The density and frequency ranges within which we have worked are such that no effects are to be expected resulting from, say, a temperature discontinuity at the walls or translational relaxation effects associated with binary molecular collisions. (Relaxation effects associated with ternary collision are mentioned below.)

6. Conclusions

The difference between our new value for the gas constant based upon acoustic measurements and that previously accepted based upon oxygen density measurements is unlikely to be explained on the basis of random errors associated with the experimental work. The two values differ by approximately eight times the standard error of our result and five times that now assigned to the previous work. We therefore conclude that a real systematic difference exists but we are unable to point to any single factor which can be unambiguously identified as the source of the disagreement.

On the basis of the present value for the gas constant, namely

$$R = \mathbf{8315.73 \pm 0.17}\,\mathrm{J\,K^{-1}\,kmol^{-1}},$$

we obtain for the normal molar volume of an ideal gas

$$V_0 = (\mathbf{22.4174 \pm 0.0005}) \times 10^{-3}\,\mathrm{m^3\,mol^{-1}}$$

and for the Boltzmann constant

$$k = (\mathbf{1.38088 \pm 0.00003}) \times 10^{-23}\,\mathrm{J\,K^{-1}}$$

using the value for the Avogadro constant N_A

$$N_A = \mathbf{6.022045} \times 10^{23}\,\mathrm{mol^{-1}}.$$

The second radiation constant of the Planck equation, $c_2 = hc/k$ becomes

$$c_2 = (\mathbf{1.43856 \pm 0.00003}) \times 10^{-2}\,\mathrm{mK}$$

and the Stefan–Boltzmann constant $\sigma = 2\pi^5 k^4/15h^3c^2$:

$$\sigma = (\mathbf{5.6739 \pm 0.0005}) \times 10^{-8}\,\mathrm{W\,m^{-2}\,K^{-4}}.$$

This value of the Stefan–Boltzmann constant differs by a substantial amount, 0.06 %, from the previous value as a consequence of the Boltzmann constant appearing to the fourth power.

The latest experimental measurements of the Stefan–Boltzmann constant (Blevin & Brown 1971) resulted in a value of $(5.6644 \pm 0.0075) \times 10^{-8}\,\mathrm{W\,m^{-2}\,K^{-4}}$. This result was obtained from measurements of the total radiation emitted from a blackbody at the freezing point of gold. The thermodynamic temperature assigned to the gold point is 1337.58 K (1064.43 °C). The difference

PHILOSOPHICAL TRANSACTIONS OF THE ROYAL SOCIETY A MATHEMATICAL, PHYSICAL & ENGINEERING SCIENCES
PHILOSOPHICAL TRANSACTIONS OF THE ROYAL SOCIETY A MATHEMATICAL, PHYSICAL & ENGINEERING SCIENCES

Downloaded from rsta.royalsocietypublishing.org

between the value of σ obtained experimentally by Blevin and that deduced using our new value of R would be completely accounted for by decrease of 0.55 K in the thermodynamic temperature assigned to the gold point. Such a decrease is by no means inconsistent with that already suggested by an extrapolation of preliminary results of gas thermometer and radiation thermometer work currently in progress in national standards laboratories (Guildner & Edsinger 1973).

The velocity of sound at n.t.p. can also be deduced from the isotherm. We find a value of

$$c_{\text{n.t.p}} = 307.853 \pm 0.004\,\text{m s}^{-1}.$$

Unfortunately the comparison of our work with past measurements is not very straightforward. A precise measurement of $c_{\text{n.t.p.}}$ (presumed to be ultrasonic) by Greenspan has not been fully reported as far as we are aware but is quoted in N.B.S. (1955) as

$$c_{\text{n.t.p}} = 307.86\,\text{m s}^{-1},$$

in excellent agreement with our own value. Another careful determination by Smith & Harlow (1963) poses difficulties of comparison because it was made at 30 °C and 10^5 Pa (1 atm) pressure. They convert their value to n.t.p. and if we correct this conversion to IPTS-68 it becomes

$$c_{\text{n.t.p.}} = 307.84\,\text{m s}^{-1}.$$

However, we are unwilling to attach very great weight to the good agreement here with our own value and that of Greenspan since there remain difficulties about the reliability of the changes in

TABLE 9. COMPARISON WITH OTHER WORK ON THE VELOCITY OF SOUND IN ARGON

source	method	no. of points and pressure range / atm	frequency / kHz	best representation of data	c_0^2(m^2 s^{-2})	$10^4\,A_1(T)$	$10^{11}\,A_2(T)$	$10^{18}\,A_3(T)$
present work	low frequency variable path interferometry	98 0.3–2.0	5.6	quadratic	94771.0 ± 2.0	0.16 ± 0.37	76.0 ± 15.5	—
Van Itterbeek, Van Dael & Grevendonk (1959)	ultrasonic inferometry	11 2.1–70.8	~ 500	cubic	94603.3 ± 87.0 (corrected to 273.16 K from 273.75 K)	5.69 ± 1.09	−4.32 ± 3.53	9.24 ± 3.15
Lestz (1963)	low frequency variable path travelling wave phase measurement in tube	7 1.0–11.9	~ 2.5	cubic	94984.7 ± 8.0 (corrected to 273.16 K from 273.15 K)	6.42 ± 5.72	−80.1 ± 10.6	3.67 ± 5.45
El Hakeem (1965)	low frequency; effectively a variable frequency interferometer with small moving microphone probe	5 1.0–70.0	2.8–4.5	quadratic	94900.9 ± 39.0 (corrected to 273.16 K from 273.15 K)	2.10 ± 0.29	6.07 ± 0.39	—
as calculated here from N.B.S. (1969)	from high pressure p.v.t. data	—	—	—	—	1.41 ± 3.12	4.59 ± 3.24	—

Downloaded from rsta.royalsocietypublishing.org

the non-ideality corrections for argon between 30 °C and 0 °C (Harlow 1975). These problems are discussed more fully below. There also exist a number of other determinations of the velocity of sound in argon close to 273.15 K, but they are primarily directed towards determining isotherm slope and curvature rather than absolute velocity and are generally of considerably lower precision than those of Greenspan and Smith & Harlow. Their results are presented in table 9 where it can be seen how large their uncertainties in c_0^2 are compared with our own. Neither is a comparison of their values of $A_1(T)$ and $A_2(T)$ with ours very informative since no clear pattern emerges even as to the best order of fit to the raw data in comparable pressure ranges. In the case of El Hakeem, for example, a quadratic fit is preferable whereas the data of Van Itterbeek *et al.* (1959) calls for a cubic representation. Yet both sets of measurements cover much the same pressure range.

TABLE 10. VALUES OF THE COEFFICIENTS N_i

coefficient	value	standard deviation
N_0	$+3.166\,028\,7\times10^{-5}$	6.005×10^{-7}
N_1	$-1.093\,626\,3\times10^{-2}$	3.659×10^{-4}
N_2	$-8.198\,753\,0\times10^{-1}$	3.582×10^{-1}
N_3	$-3.228\,890\,5\times10$	3.016×10^{0}
N_4	0	0
N_5	$+1.189\,848\,5\times10^{5}$	8.693×10^{3}
N_6	$+8.589\,341\,8\times10^{-10}$	2.211×10^{-11}
N_7	$-5.699\,667\,2\times10^{-8}$	1.612×10^{-9}
N_8	0	0
N_9	$+5.867\,034\,4\times10^{-3}$	1.029×10^{-3}
N_{10}	$+7.868\,688\,8\times10^{-1}$	3.841×10^{-1}
N_{11}	$-1.399\,730\,9\times10^{2}$	3.041×10^{1}

These coefficients have been taken from N.B.S. (1969), reindexed to suit our summations and coverted to our units. For further statistical information see source.

The compatibility of the form of our isotherm with existing p.v.t. data is even less easy to establish because of the difficulties of comparison. We are aware of two anthologies of high pressure results (N.B.S. 1955, 1969) from which information on the velocity of sound in argon may be derived. In the first velocity is tabulated as a function of temperature and pressure while the second gives a polynomial expansion in T^{-1} of the p.v. virial coefficients $B(T)$ and $C(T)$, which we prefer to quote in the following form:

$$B(T) = \sum_{i=0}^{5} N_i\, T^{-i} \tag{55}$$

and

$$C(T) = \sum_{i=0}^{5} N_{i+6}\, T^{-i}, \tag{56}$$

where the coefficients are given in table 10 together with their uncertainties. These values were obtained by the fitting of functions to selected sets of p.v.t. data. From these we may calculate c^2 as a function of pressure from the following relations

$$A_1(T) = \frac{\gamma}{M}\left\{2B + \frac{4T}{3}\frac{\mathrm{d}B}{\mathrm{d}T} + \frac{4T^2}{15}\frac{\mathrm{d}^2B}{\mathrm{d}T^2}\right\}, \tag{57}$$

and

$$A_2(T) = \frac{\gamma}{RTM}\left\{\tfrac{13}{5}C + \tfrac{16}{15}T\frac{\mathrm{d}C}{\mathrm{d}T} + \tfrac{2}{15}T^2\frac{\mathrm{d}^2C}{\mathrm{d}T^2} - \tfrac{8}{5}B^2 + \tfrac{98}{45}\left(T\frac{\mathrm{d}B}{\mathrm{d}T}\right)^2 + \tfrac{8}{45}\left(T^2\frac{\mathrm{d}^2B}{\mathrm{d}T^2}\right)^2 + \tfrac{8}{15}TB\frac{\mathrm{d}B}{\mathrm{d}T} + \tfrac{4}{15}T^2B\frac{\mathrm{d}^2B}{\mathrm{d}T^2} + \tfrac{56}{45}T^3\frac{\mathrm{d}B}{\mathrm{d}T}\frac{\mathrm{d}^2B}{\mathrm{d}T^2}\right\}, \tag{58}$$

Downloaded from rsta.royalsocietypublishing.org

or, more tractably,

$$A_1(T) = \frac{\gamma}{M}\sum_{i=0}^{5} a_i N_i T^{-i} \tag{59}$$

and

$$A_2(T) = \frac{\gamma}{RTM}\sum_{i=0}^{5}\left\{b_i N_{i+6} T^{-i} + \sum_{j=0}^{5} c_{ij} N_i N_j T^{-i-j}\right\}, \tag{60}$$

where

$$a_i = 2 - \tfrac{16}{15}i + \tfrac{4}{15}i^2, \tag{61}$$

$$b_i = \tfrac{13}{5} - \tfrac{14}{15}i + \tfrac{2}{15}i^2, \tag{62}$$

and

$$c_{ij} = -\tfrac{8}{5} + \tfrac{98}{45}ij + \tfrac{8}{45}ij(i+1)(j+1) - \tfrac{8}{15}j + \tfrac{4}{15}j(j+1) - \tfrac{56}{45}ij(j+1) \tag{63}$$

and where γ takes its ideal gas value of $\frac{5}{3}$. Assuming that the uncertainties in N_i may be combined linearly (which seems to give representative uncertainties in the expansion for $B(T)$) we obtain

$$A_1(273.16\,\mathrm{K}) = (1.41 \pm 3.12) \times 10^{-4}$$

and

$$A_2(273.16\,\mathrm{K}) = (4.59 \pm 3.24) \times 10^{-11}.$$

This enables us to plot an isotherm which, normalized to our value of c_0, agrees with our own to better than twice the sum of the standard errors in our three quadratic terms. The uncertainty in the linear coefficient $A_1(T)$ calculated above is, however, so large as to place hardly any significant constraint on measured velocities at all. Tabulated velocities from the N.B.S. (1955) anthology also agree with our own, but again the estimated uncertainties are so large as to render the comparison rather vague. However the value of $A_2(T)$ calculated above does not agree with ours. This may be because the hitherto accepted value of the gas constant was presupposed in calculating the coefficients N_i of N.B.S. (1969) to govern the asymptotic behaviour of the fitted p.v.t. surface at low pressures. Certainly the data used to compile this anthology covered much higher pressures and generally much lower temperatures than in this work, so that the calculated values of $A_1(T)$ and $A_2(T)$ presuppose extrapolations into an ideal gas region well beyond the main body of data. Moreover, the complex dependence of $A_2(T)$ upon first and second derivatives of both $B(T)$ and $C(T)$ render their evaluation doubly hazardous. Consequently we do not take the disagreement between calculated and observed values of $A_2(T)$ to be significant.

Quite apart from the above considerations, recent work by Blatt (1976) has suggested that the p.v. virial expansion may not be a sound basis for deriving a corresponding acoustic virial expansion with coefficients given by equations (57) and (58). He argues that ternary molecular collisions represented in the p.v. expansion by the virial coefficient $C(T)$ may occur with a frequency less than the sound frequency if the density of the gas is sufficiently low. That being the case, the expansion for $A_1(T)$ and $A_2(T)$ might not be applicable in our frequency range, though they would be valid at sufficiently low frequencies. Blatt gives the following approximate expansion for the frequency of ternary collisions:

$$F \simeq (n/v)^2 d^5 c_0$$

where n/v is the molecular number density and d is the interaction distance for the molecules. Because of the dependence of F on the 5th power of the interaction distance, it is very sensitive to the value chosen. Dushman & Lafferty (1962) give values of the interaction distance derived by various different techniques which range from 0.24 to 0.415 nm. While the latter figure gives a value for F many times our own operating frequency, the former yields $F \approx 16.5$ kHz which is comparable. Thus, given the approximate nature of the expansion for F, it may be the case that isotherm shape is not governed entirely by the low frequency values of $A_1(T)$ and $A_2(T)$. The

Downloaded from rsta.royalsocietypublishing.org

value of the intercept would not be in error, however, since in the limit of low pressures the ratio of the rate of ternary collisions to binary collisions approaches zero. According to Blatt's theory the acoustic isotherm should approach the orthodox thermodynamic intercept horizontally at sufficiently high frequencies. This is exactly what we observe. Such an effect is difficult to see in measurements of conventional accuracy so it would not be surprising to find that it had been overlooked in the past. However, until we can assess the matter on a firmer quantitative basis, we feel that we should adopt an agnostic attitude as to whether the isotherm shape is compatible with the orthodox low frequency theory or not. Either way our intercept and hence our value of the gas constant should be correct.

The authors are pleased to acknowledge the assistance given by Dr T. Babeliowsky of the Bureau Central de Mesures Nucleaire, Geel, Belgium, who made for us the measurements of relative isotopic composition of argon. Also the authors are grateful to the Tin Research Institute who carried out the plating of the cylinder with nickel-tin, and Mr E. Pinn of the N.P.L. Workshop who so successfully lapped the piston and cylinder assembly to the very fine tolerances required. We are also pleased to acknowledge the assistance of Mr Mark Winston who spent much of his six months at N.P.L. between school and university running the computer programs for our data processing.

References

Bateucas, T. 1972 *Atomic masses and fundamental constants* (eds. Sanders, J. H. & Wapstra, A. H.), vol. 4, pp. 534–542. London, New York: Plenum.
Bateucas, T. 1952 *An. Soc. Esp. Fis. Quim.* **48**, 4.
Bateucas, T. & Garcia Malde, G. 1950 *An. Soc. Esp. Fis. Quim.* **46**, 517.
Baxter, G. P. & Starkweather, H. W. 1924 *Proc. natn. Acad. Sci. U.S.A.* **10**, 479.
Baxter, G. P. & Starkweather, H. W. 1926 *Proc. natn. Acad. Sci. U.S.A.* **12**, 699.
Blatt, J. M. 1976 *J. Phys.* A **9**, L99.
Blevin, W. R., Brown, W. J. 1971 *Metrologia* **7**, 15.
Cohen, E. R. & Taylor, B. N. 1973 *J. Phys. Chem. Ref. Data* **2**, 4.
Colclough, A. R. 1972 Thesis, University of London.
Colclough, A. R. 1973 *Metrologia* **9**, 75.
Colclough, A. R. 1976 *Acustica* **36**, 1.
Deslattes, R. D. 1976 *Atomic masses and fundamental constants* (eds. Sanders, J. H. & Wapstra, A. H.), vol. 5. London, New York: Plenum.
Dushman, S. & Lafferty, J. M. 1962 *Scientific foundations at vacuum technique*. New York: Wiley.
El Hakeem, A. S. 1965 *J. chem. Phys.* **42**, 3132.
Fritche, L. 1960 *Acustica* **10**, 199.
Guildner, L. A. & Edsinger, R. E. 1973 *J. Res. N.B.S.* **77** A, 383–389.
Hall, J. A. & Barber, C. R. 1967 *Metrologia* **3**, 78.
Harlow, R. G. 1975 (Private communication.)
Helmholtz, H. 1863 *Verhandl, naturhist, med. Ver. Heidelberg* **3**, 16.
Henry, P. S. 1931 *Proc. Phys. Soc.* **43**, 340.
Herzfeld, Karl F. 1931 *Phys. Rev.* **38**, 1011.
The International Practical Temperature Scale of 1968 1969 H.M.S.O.: National Physical Laboratory.
Kirchhoff, G. 1868 *Ann. Physik* **134**, 177.
Lestz, S. S. 1963 *J. chem. Phys.* **38**, 2830.
Mattauch, J. H. E., Wapstra, A. H. & König, L. A. 1962 *Nuclear Phys.* **31**, 1.
Melton, C. E., Massey, W. & Abels, B. N. 1971 *Z. Naturforsh.* **26**a, 1241.
Moles, E. 1938 *Collections scientifique d'Institute Internationale Coopérative Intellectuel*, pp. 1–75. Paris.
National Bureau of Standards Circular 564 1955 Washington: U.S. Government Printing Office.
National Bureau of Standards Report 27 1969 Washington: U.S. Government Printing Office.
Nier, A. O. 1950 *Phys. Rev.* **77**, 789.
Quinn, T. J. 1972 *Atomic masses and fundamental constants* (eds. Sanders, J. H. & Wapstra, A. H.), vol. 4, pp. 529–533. London, New York: Plenum.
Quinn, T. J., Chandler, T. R. D. & Colclough, A. R. 1974 *Nature, Lond.* **250**, 5463.
Schneebeli, H. 1869 *Ann. Physik* **136**, 296.

PHILOSOPHICAL TRANSACTIONS OF THE ROYAL SOCIETY A MATHEMATICAL, PHYSICAL & ENGINEERING SCIENCES
PHILOSOPHICAL TRANSACTIONS OF THE ROYAL SOCIETY A MATHEMATICAL, PHYSICAL & ENGINEERING SCIENCES

Downloaded from rsta.royalsocietypublishing.org

Schweikert, G. 1915 *Ann. Physik* **48**, 593.
Seebeck, A. 1870 *Ann. Physik* **139**, 104.
Shields, F. D., Lee, K. P. & Wiley, W. J. 1965 *J. acoust. Soc. Am.* **37**, 4.
Smith, D. H. & Harlow, R. G. 1963 *Brit. J. appl. Phys.* **14**, 102.
Stickney, R. E. & Hurlbut, F. C. 1963 *Rarified gas dynamics.* (Ed. J. A. Laurmann), vol. 1, p. 454. New York: Academic Press.
Strutt, J. W., Baron Rayleigh 1945 *The theory of sound*, vol. 1, p. 323. New York: Dover Publications.
Thiesen, M. 1907 *Ann. Physik* **24**, 401.
Van Itterbeek, A., Van Dael, W. & Grevendonk, W. 1959 *Physica* **25**, 640.
United States Bureau of Mines. 1967 Info. Circular 8317.
Weston, D. E. 1953 *Proc. Phys. Soc.* B **66**, 695.

Appendix A

The relation between admittance circles and impedance circles

The modulus of the complex mechanical impedance of the interferometer's gas loaded transducer can be directly measured in terms of the ratio driving force/particle velocity or, being a moving coil device, driving current/particle velocity. One might have chosen to hold the current constant and measure the velocity modulus, but not its phase. That being the case one would have had to take the reciprocal to give $|\boldsymbol{Z}(l)| = |\boldsymbol{Z}_{\mathrm{T}} + \boldsymbol{Z}_{\mathrm{G}}(l)| = 1/\dot{\xi}$ in arbitrary units. The impedance circles could then have been somewhat laboriously reconstructed by conventional methods from the plot of $|\boldsymbol{Z}(l)|$, i.e. from the impedance 'resonance curve' (Colclough 1973). In order to plot impedance circles directly it would have been necessary to invert the accelerometer signal electronically or, perhaps, to plot the driving current required to maintain constant velocity $\dot{\xi}$ as the resonances were scanned. In that case the drive would have to be servoed to the velocity. Clearly it is far simpler to plot particle velocity $\dot{\xi}$ at constant current, but that quantity is admittance rather than impedance. Throughout this work the theory of impedance circles has been used although in practice admittance circles were plotted. This enabled us to take advantage of the fact that admittance circles are more accessible experimentally while impedance circles are more familiar (though not conceptually any more fundamental). It now remains to show that it is possible to proceed in this apparently paradoxical way without incurring any errors. This certainly requires justification since (i) The observed position of resonances on admittance circles are different from those of the corresponding impedance circles, (ii) Their observed diameters stand in different ratios, and (iii) The measured half-widths are changed.

That the inverse of a circle in the complex plane is also a circle follows from an elementary theorem of the theory of conformal mapping. This states that a Möbius transformation, i.e. a general bilinear transformation of the form $\boldsymbol{\omega}(\boldsymbol{z}) = (\boldsymbol{pz}+\boldsymbol{q})/(\boldsymbol{sz}+\boldsymbol{t})$ where $\boldsymbol{p}$, $\boldsymbol{q}$, $\boldsymbol{s}$ and $\boldsymbol{t}$ are complex constants, transforms circles $\boldsymbol{z}$ into circles $\boldsymbol{\omega}(\boldsymbol{z})$. Such transformations are easily expressed as a combination of translation, rotation, expansion and inversion which are all special cases of the general Möbius transformation. In particular the inversion $\boldsymbol{\omega}(\boldsymbol{z}) = \boldsymbol{z}^{-1}$ is seen to occur when $\boldsymbol{p} = \boldsymbol{t} = 0$ and $\boldsymbol{q} = \boldsymbol{s}$. Thus the figure obtained as the complex reciprocal of an impedance circle will also be a circle – an 'admittance' circle. The trivially obvious invariance of circularity under expansion explains why circular figures were still obtained when arbitrary units were employed and, equally trivially, the invariance under rotation explains why they were obtained when no effort was made to orientate the figures correctly in the complex plane, i.e. why it was possible to ignore constant phase and amplitude factors such as $i\omega$ when plotting them. Similarly, invariance under translation is bound up with being able to ignore the location, $\boldsymbol{Z}_{\mathrm{T}}$, of the figures in the complex plane. The last three matters can be taken for granted, but the preservation of

Downloaded from rsta.royalsocietypublishing.org

circularity under inversion will be proved, admittance circle diameters and centres being derived in the process.

Expressing the circle to be inverted by the general form for a circle, one has

$$a\boldsymbol{z}\boldsymbol{z}^* - \boldsymbol{b}^*\boldsymbol{z} - \boldsymbol{b}\boldsymbol{z}^* + c = 0 \tag{A 1}$$

where a and c are real constants, a being non-zero for a finite radius, and $\boldsymbol{b}$ is a complex constant such that $\boldsymbol{b}/a$ represents the centre. For an impedance circle of order N, $\boldsymbol{b}/a$ becomes†

$$\boldsymbol{b}_N/a = (R_T + \tfrac{1}{2}D_N) + \mathrm{i}X_T. \tag{A 2}$$

In general the circle radius, r, appears in equation (A 1) through the constant c which is given by $c/a = (\boldsymbol{b}\boldsymbol{b}^*/a^2) - r^2$ or, for an impedance circle,

$$c_N/a = (\boldsymbol{b}_N \boldsymbol{b}_N^*)/a^2 - \tfrac{1}{4}D_N^2. \tag{A 3}$$

If $\boldsymbol{\omega} = \boldsymbol{z}^{-1}$ then equation (A 1) yields

$$c\boldsymbol{\omega}\boldsymbol{\omega}^* - \boldsymbol{b}\boldsymbol{\omega} - \boldsymbol{b}^*\boldsymbol{\omega}^* + a = 0, \tag{A 4}$$

which, having the same form, must also be a circle as asserted. Comparison of coefficients enables the centre of the admittance circle to be identified as $\boldsymbol{b}^*/c$ which, from equations (A 2) and (A 3), is given by

$$\frac{\boldsymbol{b}_N^*}{c_N} = \frac{(R_T + \tfrac{1}{2}D_N) - \mathrm{i}X_T}{Z_T^2 + R_T D_N} \tag{A 5}$$

for the Nth admittance circle. The admittance circle equation corresponding to equation (A 3) is

$$a/c_N = (\boldsymbol{b}_N \boldsymbol{b}_N^*)/c^2 - \tfrac{1}{4}D_N^{(A)2} \tag{A 6}$$

where $D_N^{(A)}$ is the diameter of the Nth admittance circle. From equations (A 3) and (A 5) this yields an expression for $D_N^{(A)}$:

$$D_N^{(A)} = \frac{D_N}{Z_T^2 + R_T D_N}. \tag{A 7}$$

Thus one has in equations (A 5) and (A 7) the information necessary to plot the admittance circle corresponding to any impedance circle as shown in figure A 1. There it can be seen that the phase $\phi_N^{(A)}$ on the admittance circle at $l = l_N$ is not zero as in the case of the impedance circle. One measures instead a value $l = l_N^{(A)}$ corresponding to $\phi_N^{(A)} = 0$, i.e. for which the point describing the admittance circle is diametrically opposite its antiresonance, $\boldsymbol{Z}_T^{-1}$. Similarly half widths would be obtained as half the change in l required to traverse the admittance circle from $\phi_N^{(A)} = +\tfrac{1}{4}\pi$ to $-\tfrac{1}{4}\pi$. It is in principle a simple, but tedious, exercise in coordinate geometry to derive the impedance circle phases, ϕ_N, corresponding to $\phi_N^{(A)} = +\tfrac{1}{4}\pi$, 0 and $-\tfrac{1}{4}\pi$. They are given by

$$\phi_N^{(A)} = 0: \quad \tan\phi_N = -\frac{X_T D_N}{Z_T^2}, \tag{A 8}$$

$$\phi_N^{(A)} = \pm\tfrac{1}{4}\pi: \quad \tan\phi_N = \pm 1 \pm \frac{(R_T \mp X_T) D_N}{Z_T^2}. \tag{A 9}$$

The most convenient way to derive a general relation between ϕ_N and $\phi_N^{(A)}$ is to use another elementary theorem of conformal mapping theory which states that under a Möbius transformation the 'cross product', $\chi = (\boldsymbol{z}_4 - \boldsymbol{z}_1)(\boldsymbol{z}_2 - \boldsymbol{z}_3)/(\boldsymbol{z}_2 - \boldsymbol{z}_1)(\boldsymbol{z}_4 - \boldsymbol{z}_3)$, of the four distinct points $\boldsymbol{z}_1$ to $\boldsymbol{z}_4$ is invariant. In particular for four such points on an impedance (or admittance) circle

$$\frac{(\boldsymbol{z}_4 - \boldsymbol{z}_1)(\boldsymbol{z}_2 - \boldsymbol{z}_3)}{(\boldsymbol{z}_2 - \boldsymbol{z}_1)(\boldsymbol{z}_4 - \boldsymbol{z}_3)} = \frac{(\boldsymbol{z}_4^{-1} - \boldsymbol{z}_1^{-1})(\boldsymbol{z}_2^{-1} - \boldsymbol{z}_3^{-1})}{(\boldsymbol{z}_2^{-1} - \boldsymbol{z}_1^{-1})(\boldsymbol{z}_4^{-1} - \boldsymbol{z}_3^{-1})}. \tag{A 10}$$

† In what follows R_T aud X_T will be taken to be dimensionless in conformity with our setting $D_N = (\alpha l_N + \beta)^{-1}$, Δ_N retaining the dimension of length. Dimensional homogeneity is obtained by restoring the factor $\pi b^2 \rho c$ to D_N.

Downloaded from rsta.royalsocietypublishing.org

These ratios are particularly tractable in calculation since they involve only differences in positions of points on the circles and so may be evaluated irrespective of the positions of the circles in the complex plane. Taking $\boldsymbol{z}_1^{-1}$ to be a variable point, z^{-1}, of phase $\phi^{(A)}$ on the admittance circle and $\boldsymbol{z}_2^{-1}$, $\boldsymbol{z}_3^{-1}$ and $\boldsymbol{z}_4^{-1}$ to be respectively $\boldsymbol{Z}_T^{-1}$, that value of z^{-1} for which $\phi^{(A)} = -\frac{1}{4}\pi$ and that for which $\phi^{(A)} = 0$ (see figure A 2), one finds

$$\chi = \mathrm{i}\left(\frac{z_4^{-1} - z^{-1}}{z_2^{-1} - z^{-1}}\right) \times \mathrm{i}\left(\frac{z_2^{-1} - z_3^{-1}}{z_4^{-1} - z_3^{-1}}\right) = -\tan\phi^{(A)} \tan\tfrac{1}{4}\pi = -\tan\phi^{(A)}, \tag{A 11}$$

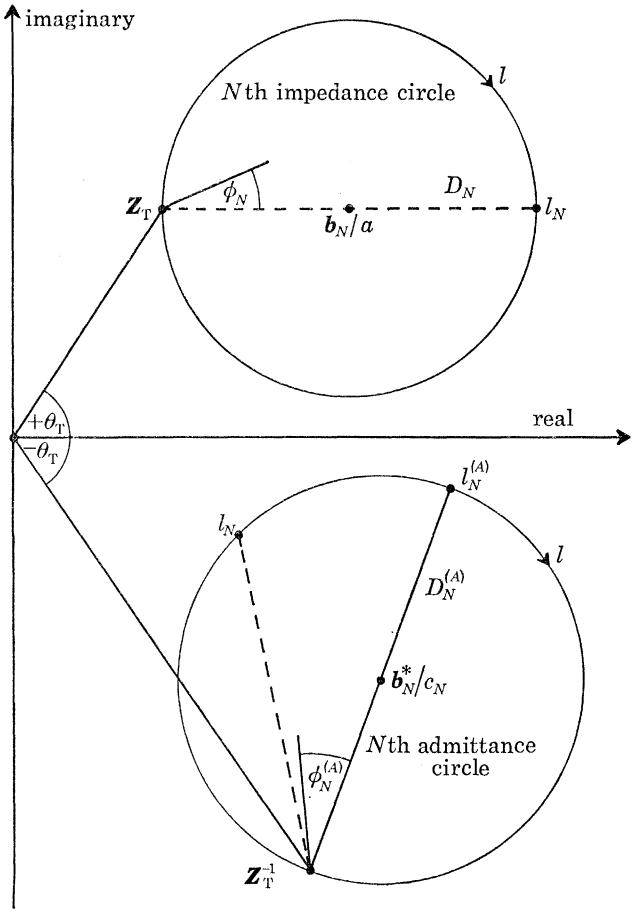

FIGURE A 1. The relation of an admittance circle to its corresponding impedance circle.

where the orthogonality of angles in a semicircle has enabled the factors i to be extracted. This is a particularly felicitous result since it shows that the quantity of interest, $\tan\phi^{(A)}$, may be set directly equal to the cross product χ evaluated on the impedance circle. Measuring phases ϕ relative to antiresonance ($\boldsymbol{z}_2 = 0$) one has $\boldsymbol{z}_j = D_N \cos\phi_j \exp(\mathrm{i}\phi_j)$ where $j = 1$, 3 and 4 which gives after some trigonometric manipulation

$$\chi = \frac{\tan\phi_1 - \tan\phi_4}{\tan\phi_3 - \tan\phi_4} \tag{A 12}$$

(the subscripts of ϕ referring to j and not, of course, to N). Or, from equations (A 8), (A 9) and (A 11)

$$\tan\phi_N^{(A)} = \frac{\tan\phi_N + X_T D_N/Z_T^2}{1 + R_T D_N/Z_T^2} \tag{A 13}$$

Downloaded from rsta.royalsocietypublishing.org

(reverting to the original subscripts, N), If we write $\tan\phi_N = (l_N - l)/\Delta_N$ this yields directly

$$\tan\phi_N^{(A)} = \frac{l_N^{(A)} - l}{\Delta_N^{(A)}}, \tag{A 14}$$

where

$$l_N^{(A)} = l_N + X_T D_N \Delta_N / Z_T^2 \tag{A 15}$$

$$= l_N + X_T/(kZ_T^2)$$

and

$$\Delta_N^{(A)} = \Delta_N(1 + R_T D_N/Z_T^2)$$

$$= \frac{\alpha l_N + (\beta + R_T/(Z_T^2))}{k}, \tag{A 16}$$

thus displaying a broad formal analogy with the corresponding fundamental first order relations for impedance circles. These relations immediately reveal why no error arises in the measured value of sound velocity when admittance circles are treated as impedance circles even though $l_N^{(A)} \neq l_N$. In a variable path device it is the separation of resonance positions, l_N or $l_N^{(A)}$, which are measured. Since equation (A 15) shows them all to have been changed by the same amount their separations remain unchanged. Equation (A 16) implies that if attempts are made to determine α and β from several measured values of $\Delta_N^{(A)}$, then α will be correctly determined but β will not be.

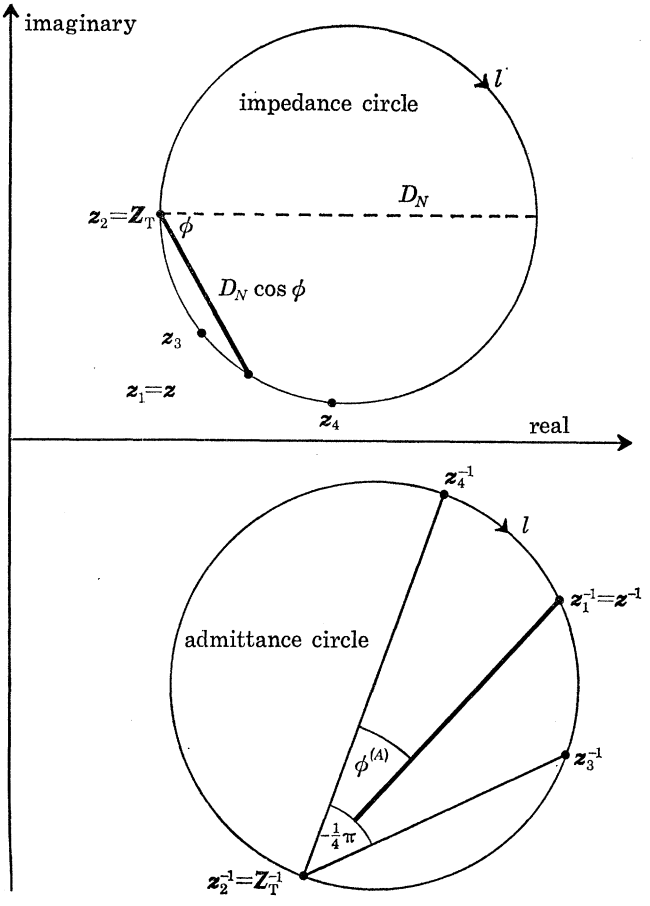

FIGURE A 2. Location of z_j for $j = 1, 2, 3$ and 4.

Downloaded from rsta.royalsocietypublishing.org

Instead one obtains

$$\beta^{(A)} = \beta + R_T/(Z_T^2). \tag{A 17}$$

This is of no consequence in the present work since no need has arisen to determine β. However, it is necessary to ensure that no errors arise in measured values of α when, as in our case, it is determined from measured values both of $D_N^{(A)}$ and $\Delta_N^{(A)}$. From equation (A 7) one has

$$1/D_N^{(A)} = (\alpha Z_T^2)\, l_N + (\beta Z_T^2 + R_T). \tag{A 18}$$

Thus instead of determining a loss ratio $\mu = \alpha/\beta$ one obtains

$$\mu^{(A)} = \frac{\mu}{1 + R_T/(\beta Z_T^2)}. \tag{A 19}$$

So calculating α from $\mu^{(A)}$ and $\Delta_N^{(A)}$gives

$$\begin{aligned} \alpha^{(A)} &= k\Delta_N^{(A)}/(l_N + 1/\mu^{(A)}) \\ &= \alpha \end{aligned} \tag{A 20}$$

as required (by substituting for $\Delta_N^{(A)}$ and $\mu^{(A)}$ from equations (A 16) and (A 19) respectively). This completes the justification of our use of impedance circle theory when treating admittance circles.

Appendix B

The effect of approximations in the first order theory of the acoustic interferometer

The fundamental relations for the impedance, $\boldsymbol{Z}_G(l)$, loading the transducer of a variable path interferometer are, without approximations,

$$\boldsymbol{Z}_G(l) = (1 - i\alpha/k)\, R_T^{\frac{1}{2}} \left\{ \frac{1 + R_R\, e^{-2\alpha l}\, e^{-2ikl}}{1 - R_R R_T\, e^{-2\alpha l}\, e^{-2ikl}} \right\} = (1 - i\alpha/k)\,(R(l) - iX(l)) \tag{B 1}$$

in units of $\pi b^2 \rho c$ where

$$R(l) = R_T^{\frac{1}{2}} \left\{ \frac{1 - R_R^2 R_T\, e^{-4\alpha l} + R_R(1 - R_T)\, e^{-2\alpha l} \cos 2kl}{1 + R_R^2 R_T^2\, e^{-4\alpha l} - 2R_R R_T\, e^{-2\alpha l} \cos 2kl} \right\} \tag{B 2}$$

and

$$X(l) = R_T^{\frac{1}{2}} \left\{ \frac{R_R(1 + R_T)\, e^{-2\alpha l} \sin 2kl}{1 + R_R^2 R_T^2\, e^{-4\alpha l} - 2R_R R_T\, e^{-2\alpha l} \cos 2kl} \right\}. \tag{B 3}$$

These relations may be derived by summing the positive and negative going waves which arise in the cavity due to the transducer vibration at $z = l$ whose displacement is assumed to be $\xi(l) = \xi_0 \exp(i\omega t)$. The factors $R_T^{\frac{1}{2}}$ arise because mechanisms which result in a reflexion coefficient R_T act in such a way as to give an 'emission coefficient', $R_T^{\frac{1}{2}}$, when the corresponding surface vibrates.

Nearly always the factor $(1 - i\alpha/k)$ in equation (B 1) is set equal to one since $\alpha \ll k$ is a necessary condition for sensitive interferometry implying that no significant attenuation occurs in distances of the order of a wavelength. Even when this is done one cannot necessarily regard $R(l)$ and $-X(l)$ as real and imaginary parts of $\boldsymbol{Z}_G(l)$ since R_R or R_T may be complex signifying that reflexion at R or T is accompanied by a phase change as well as a reflexion loss. In this work two simplifying assumptions have been made: (i) $R_R = R_T = R \equiv (1 - \beta)$, all values being real, and (ii) The quantities αl, β and, in the neighbourhood of resonance, $2k(l_N - l)$ are small enough to render terms of order two or higher in them negligible *in comparison* (in particular $(1 - i\alpha/k) = 1$

Downloaded from rsta.royalsocietypublishing.org

as usual). Assumption (ii) constitutes the 'first order' approximation employed by most workers which, with assumption (i) leads to the following very simple and perspicuous basic relations:

$$Z_{\mathrm{G}}(l) = R(l) - \mathrm{i}X(l), \tag{B 4}$$

$$R(l) = \frac{D_N}{1+((l_N-l)/\Delta_N)^2} \tag{B 5}$$

and

$$X(l) = \frac{D_N((l_N-l)/\Delta_N)}{1+((l_N-l)/\Delta_N)^2}, \tag{B 6}$$

where the small quantity

$$\Delta_N \equiv (\alpha l_N+\beta)/k \tag{B 7}$$

and the large one

$$D_N \equiv (\alpha l_N+\beta)^{-1}. \tag{B 8}$$

Here $R(l)$ and $-X(l)$ are the real and imaginary parts of $\boldsymbol{Z}_{\mathrm{G}}(l)$, and their form is easily identifiable by inspection. In particular D_N and Δ_N are seen to be the maximum and half width of $R(l)$ respectively. One also sees that the locus of $Z_{\mathrm{G}}(l)$ is a circle of diameter D_N centred at $\boldsymbol{Z}_{\mathrm{T}}+\frac{1}{2}D_N$ in the complex plane since

$$(R(l)-D_N/2)^2+X^2(l) = (D_N/2)^2. \tag{B 9}$$

This locus may not be an accurate representation of $\boldsymbol{Z}_{\mathrm{G}}(l)$ in the region of antiresonance, however, because it was assumed that $2k(l_N-l) \ll 1$. A straightforward first order analysis of $\boldsymbol{Z}_{\mathrm{G}}(l)$ shows that at antiresonance $X(l) = 0$ and $R(l) = \alpha l+\frac{1}{2}\beta_{\mathrm{R}}$ whereas the circle (B 9) passes through $X(l) = R(l) = 0$. But since $\alpha l+\frac{1}{2}\beta_{\mathrm{R}}$ is of the second order of smallness compared to the circle diameter D_N it may be ignored thus vindicating the general assumption of circularity in the first order theory. The fundamental phase relation $\tan\phi_N = -X(l)/R(l) = (l_N-l)/\Delta_N$ follows directly from equations (B 5) and (B 6). The employment of these relations will now be vindicated by showing that in variable path interferometry it is perfectly permissable to assume that R_{R} and R_{T} are real and equal even if they are not and by deriving analogous relations to those of the first order which are accurate to second order, i.e. which neglect only terms of order three and higher in the small quantities αl, β and $2k(l_N-l)$ in comparison to the quantities themselves.

Intuitively it is easy to see what effect complex values of R_{R} and R_{T} will have. If a wave is reflected from a surface at z_0 with a phase change $\pm\delta$, it is as though it were reflected from an imaginary surface at $z_0 \pm \delta/2k$. Thus in such cases it should be possible to replace the true geometrical length of the cavity by an effective length given by

$$l_{\mathrm{eff}} = l \pm (\delta_{\mathrm{R}}+\delta_{\mathrm{T}})/2k. \tag{B 10}$$

This effective length would only be expected to replace l in the 'interference' terms $\sin 2kl$ and $\cos 2kl$ of equations (B 2) and (B 3). In the 'transmission loss' terms $\exp(-2\alpha l)$ and $\exp(-4\alpha l)$ the geometrical value, l, should be retained since it represents the actual distance over which attenuation occurred (which obviously could not include imaginary displacements $\pm\delta/2k$). Replacing R_{R} and R_{T} by $R_{\mathrm{R}}\exp(\pm\mathrm{i}\delta_{\mathrm{R}})$ and $R_{\mathrm{T}}\exp(\pm\mathrm{i}\delta_{\mathrm{T}})$ respectively in equation (B 1), one has

$$Z_{\mathrm{G}}(l) = (1-\mathrm{i}\alpha/k)\,R_{\mathrm{T}}^{\frac{1}{2}}\,\mathrm{e}^{\pm\mathrm{i}\delta_{\mathrm{T}}/2}\left\{\frac{1+R_{\mathrm{R}}\,\mathrm{e}^{-2\alpha l}\,\mathrm{e}^{-\mathrm{i}(2kl\mp\delta_{\mathrm{R}})}}{1-R_{\mathrm{R}}R_{\mathrm{T}}\,\mathrm{e}^{-2\alpha l}\,\mathrm{e}^{-\mathrm{i}(2kl\mp\delta_{\mathrm{R}}\mp\delta_{\mathrm{T}})}}\right\}$$

$$\doteq (1-\mathrm{i}\alpha/k)\,R_{\mathrm{T}}^{\frac{1}{2}}\left\{\frac{1+R_{\mathrm{R}}\,\mathrm{e}^{-2\alpha l}\,\mathrm{e}^{-\mathrm{i}2kl_{\mathrm{eff}}}}{1-R_{\mathrm{R}}R_{\mathrm{T}}\,\mathrm{e}^{-2\alpha l}\,\mathrm{e}^{-\mathrm{i}2kl_{\mathrm{eff}}}}\right\}, \tag{B 11}$$

Downloaded from rsta.royalsocietypublishing.org

an expression accurate to second order and of the predicted form. Moreover, it is possible now to write $R_R \exp(-2\alpha l) = R'_R \exp(-2\alpha l_{eff})$ where $R'_R = R_R(1 \pm \alpha(\delta_l + \delta_T)/k)$ thus replacing all occurrences of l in equation (B 1) by l_{eff} so implying that resonance occurs at $l_{eff} = N\lambda/2$ or $l = l_N \pm (\delta_R + \delta_T)/2k$ as in the intuitive equation (A 10). This shows that each position of resonance is shifted by the same amount $\pm(\delta_R + \delta_T)/2k$ so that the measured separations of the positions of resonance remain unchanged. Thus it is possible to ignore end face phase changes in variable path interferometry both to first and second order.

If one proceeds on the basis of assumption (ii), but not assumption (i), exactly the same basic first order relations are obtained except that $\Delta_N = \alpha l_N + \beta$ becomes $\Delta_N = \alpha l_N + \frac{1}{2}(\beta_R + \beta_T)$ where $\beta_R = 1 - R_R$ and $\beta_T = 1 - R_T$ (taking R_R and R_T to be real again). Thus β may be regarded as standing either for a common end face reflexion loss or for the average end face reflexion loss. Since no occasion arose to distinguish between β_R and β_T and since measurement of α and c proceeds in the same way irrespective of the interpretation of β, it is perfectly harmless to ignore any difference between R_R and R_T. The use of assumption (i) has therefore been justified to first order.

To second order the expressions for $R(l)$ and $X(l)$ become

$$R(l) = \frac{D_N - (2\alpha^2 l_N^2 + 2\alpha l_N(\beta_R + \beta_T) + \beta_R\beta_T + (\beta_R^2 + \beta_T^2)/4)\, D_N^2 - \alpha/k\,((l_N - l)/\Delta_N)\, D_N}{1 - (2\alpha^2 l_N^2 + 2\alpha l_N(\beta_R + \beta_T) + \beta_R\beta_T)\, D_N + ((l_N - l)/\Delta_N)^2\,(1 - 2/D_N) - 2\alpha/k\,((l_N - l)/\Delta_N)} \tag{B 12}$$

and

$$X(l) = \frac{(1 - 2/D_N)\, D_N\,((l_N - l)/\Delta_N)}{1 - (2\alpha^2 l_N^2 + 2\alpha l_N(\beta_R + \beta_T) + \beta_R\beta_T)\, D_N + ((l_N - l)/\Delta_N)\,(1 - 2/D_N) - 2\alpha/k\,((l_N - l)/\Delta_N)}. \tag{B 13}$$

Writing equation (B 1) as

$$\boldsymbol{Z}_G(l) = \left\{R(l)\left(1 - \frac{\alpha}{k}\frac{X(l)}{R(l)}\right) - iX(l)\left(1 + \frac{\alpha}{k}\frac{R(l)}{X(l)}\right)\right\} \tag{B 14}$$

and noting that (B 12) and (B 13) imply that

$$\left\{R(l)\left(1 - \frac{\alpha}{k}\frac{X(l)}{R(l)}\right) - \frac{D_N^{II}}{2}\right\}^2 + \left\{X(l)\left(1 + \frac{\alpha}{k}\frac{R(l)}{X(l)}\right)\right\}^2 = \left\{\frac{D_N^{II}}{2}\right\}^2, \tag{B 15}$$

where

$$D_N^{II} = D_N\left\{1 - \frac{\beta_R^2 + \beta_T^2}{4} D_N\right\} \tag{B 16}$$

it can be seen that the locus of $\boldsymbol{Z}_G(l)$ remains circular in the second order theory. The circle diameter is D_N^{II} to second order and its centre is at $\boldsymbol{Z}_T + \frac{1}{2}D_N^{II}$. Again the derivation is not strictly valid close to antiresonance, but, as in the first order approximation, may still be assumed to be so, since $R(l)$ was two orders of smallness less than the circle diameter (cf. first order correction in equation (B 16)).

The fundamental second order equations yield for the observed circle phase

$$\tan\phi_N^{II} = \left(1 - \frac{\beta_R^2 + \beta_T^2}{4} D_N\right)\left(\frac{l_N - l}{\Delta_N}\right) - \frac{\alpha}{k}. \tag{B 17}$$

Clearly if the value of l_N is determined from that value of l for which $\tan\phi_N^{II} = 0$ an error of $\alpha\Delta_N/k$ will result. Since the position of both the first and the last resonance (the Mth, say) will be in error by this amount, their separation, and hence the measured velocity of sound, will be in

Downloaded from rsta.royalsocietypublishing.org

error by a fraction $2(\alpha/k)\,(\Delta_M-\Delta_1)/((M-1)\,\lambda)$. Thus measured values of c should be increased by the following minute correction

$$\Delta c/c = (\alpha/k)^2. \tag{B 18}$$

Similarly if measured half widths are determined from the change in l necessary to change $\tan\phi_N^{\mathrm{II}}$ from $+1$ to -1 the value obtained will be

$$\Delta_N^{\mathrm{II}} = \Delta_N\left(1+\frac{\beta_{\mathrm{R}}^2+\beta_{\mathrm{T}}^2}{4}D_N\right), \tag{B 19}$$

which suggests that one should write the second order phase relation in a form analogous to that for the first order theory:

$$\tan\phi_N^{\mathrm{II}} = \left(\frac{l_N^{\mathrm{II}}-l}{\Delta_N^{\mathrm{II}}}\right), \tag{B 20}$$

where

$$l_N^{\mathrm{II}} = l_N-\frac{\alpha}{k}\Delta_N, \tag{B 21}$$

and Δ_N^{II} is given by equation (B 19). In spite of the first order changes in measured values of half widths and circle diameters, it can be shown that measured values of α were exact when derived in the basis of the first order relation. Equation (B 16) may be written

$$1/D_N^{\mathrm{II}} = \alpha l_N+\beta^{\mathrm{II}}, \tag{B 22}$$

where

$$\beta^{\mathrm{II}} = \frac{\beta_{\mathrm{R}}+\beta_{\mathrm{T}}}{2}+\frac{\beta_{\mathrm{R}}^2+\beta_{\mathrm{T}}^2}{4}. \tag{B 23}$$

Hence the loss ratio measured from circle diameters is really

$$\mu^{\mathrm{II}} \equiv \alpha/\beta^{\mathrm{II}}, \tag{B 24}$$

which yields

$$\alpha^{\mathrm{II}} = k\Delta_N^{\mathrm{II}}/(l_N+1/\mu^{\mathrm{II}})$$
$$= \alpha$$

as asserted. The above analysis also shows that assumption (i) holds good for purposes of a second order analysis of the variable path interferometer since these results have been obtained without assuming $\beta_{\mathrm{R}} = \beta_{\mathrm{T}}$.

Exactly analogous arguments may be applied to a second order analysis of admittance circles. One finds

$$\tan\phi^{(\mathrm{II}A)} = \frac{l_N^{(\mathrm{II}A)}-l}{\Delta_N^{(\mathrm{II}A)}}, \tag{B 25}$$

where

$$l_N^{(\mathrm{II}A)} = l_N^{\mathrm{II}}-\frac{X_{\mathrm{T}}}{kZ_{\mathrm{T}}^2}, \tag{B 26}$$

$$\Delta_N^{(\mathrm{II}A)} = \Delta_N^{\mathrm{II}}(1+R_{\mathrm{T}}D_N^{\mathrm{II}}/Z_{\mathrm{T}}^2), \tag{B 27}$$

and

$$D_N^{(\mathrm{II}A)} = \frac{D_N^{\mathrm{II}}}{Z_{\mathrm{T}}^2+R_{\mathrm{T}}D_N^{\mathrm{II}}}. \tag{B 28}$$

Again it transpires that the minute fractional correction $\Delta c/c = (\alpha/k)^2$ has to be applied to c, but that α is exact.

To summarize: no error arises in using the simple first order theory of the text when calculating absorption coefficients and making boundary layer corrections. This is true both for impedance

Downloaded from rsta.royalsocietypublishing.org

and admittance circle measurements. But when using impedance or admittance circles to measure velocity a small fractional error of $-(\alpha/k)^2$ arises.

In the present work α was found to be $1.75 \times 10^{-3}\,\mathrm{cm}^{-1}$ at 100 kPa and $3.20 \times 10^{-3}\,\mathrm{cm}^{-1}$ at 30 kPa. The fractional velocity errors would therefore be 2.3 and 7.8 p.p.m. respectively. Extrapolating this error to zero pressure one finds a fractional decrease in c_0 of 10.2 p.p.m. or 20.4 p.p.m. in the gas constant. The corrections were made to each point before fitting the isotherm, but this figure represents an estimate of what effect they have on our final answer.

We see no reason why having made this correction our acoustic interferometry should not be free of systematic errors. But it should be borne in mind that this type of instrument is not generally used to accuracies approaching $(\alpha/k)^2$. Indeed we know of no previous work where accuracies have been demanded to the 1–10 p.p.m. level rather than the more usual 100 p.p.m. level. Thus having made the above correction for second order effects we have considered quoting a further systematic uncertainty at 20 p.p.m. in the gas constant simply as a measure of suspicion in recognition of the fact that the technique has been pressed beyond its normal range of well tried application. However, we have refrained from doing so since in the absence of any hard and fast knowledge of a further source of uncertainty such a precaution might be misleading as well as unnecessary.

PHILOSOPHICAL TRANSACTIONS OF THE ROYAL SOCIETY A MATHEMATICAL, PHYSICAL & ENGINEERING SCIENCES

PHILOSOPHICAL TRANSACTIONS OF THE ROYAL SOCIETY A MATHEMATICAL, PHYSICAL & ENGINEERING SCIENCES

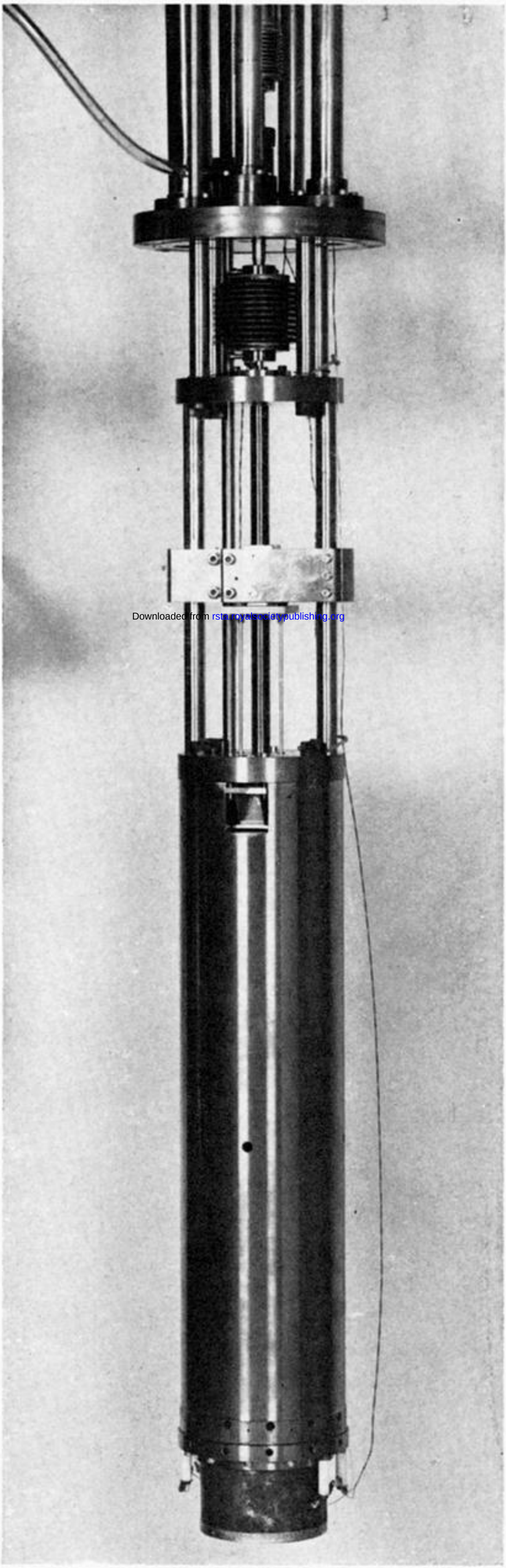

Downloaded from rsta.royalsocietypublishing.org

FIGURE 8. The acoustic interferometer assembly.

PHILOSOPHICAL TRANSACTIONS OF THE ROYAL SOCIETY A MATHEMATICAL, PHYSICAL & ENGINEERING SCIENCES

PHILOSOPHICAL TRANSACTIONS OF THE ROYAL SOCIETY A MATHEMATICAL, PHYSICAL & ENGINEERING SCIENCES